Summer 8-31-2005

Haptic induced motor learning and the extension of its benefits to stroke patients

Adrienne M. Coppa
New Jersey Institute of Technology

Copyright Warning & Restrictions

The copyright law of the United States (Title 17, United States Code) governs the making of photocopies or other reproductions of copyrighted material.

Under certain conditions specified in the law, libraries and archives are authorized to furnish a photocopy or other reproduction. One of these specified conditions is that the photocopy or reproduction is not to be "used for any purpose other than private study, scholarship, or research." If a, user makes a request for, or later uses, a photocopy or reproduction for purposes in excess of "fair use" that user may be liable for copyright infringement,

This institution reserves the right to refuse to accept a copying order if, in its judgment, fulfillment of the order would involve violation of copyright law.

Please Note: The author retains the copyright while the New Jersey Institute of Technology reserves the right to distribute this thesis or dissertation

Printing note: If you do not wish to print this page, then select "Pages from: first page # to: last page #" on the print dialog screen

ABSTRACT

HAPTIC INDUCED MOTOR LEARNING AND THE EXTENSION OF ITS BENEFITS TO STROKE PATIENTS

by
Adrienne M. Coppa

In this research, the Haptic Master robotic arm and virtual environments are used to induce motor learning in subjects with no known musculoskeletal or neurological disorders. It is found in this research that both perception and performance of the subject are increased through the haptic and visual feedback delivered through the Haptic Master. These system benefits may be extended to enhance therapies for patients with loss of motor skills due to neurological disease or brain injury.

Force and visual feedback were manipulated within virtual environment scenarios to facilitate learning. In one force feedback condition, the subject is required to maneuver a sphere through a haptic maze or linear channel. In the second feedback condition, the subject's movement was stopped when the sphere came in contact with the haptic walls. To resume movement, the force vector had to be redirected towards the optimal trajectory. To analyze the efficiency of the various scenarios, the area between the optimal and actual trajectories was used as a measure of learning.

The results from this research demonstrated that within more complex environments one type of force feedback was more successful in facilitating motor learning. In a simpler environment, two out of three subjects experienced a higher degree of motor learning with the same type of force feedback. Learning is not enhanced with the presence of visual feedback. Also, in nearly all studied cases, the primary limitation to learning is shoulder and attention fatigue brought on by the experimentation.

HAPTIC INDUCED MOTOR LEARNING AND THE EXTENSION OF ITS BENEFITS TO STROKE PATIENTS

by
Adrienne M. Coppa

A Thesis
Submitted to the Faculty of
New Jersey Institute of Technology
in Partial Fulfillment of the Requirements for the Degree of
Master of Science in Biomedical Engineering

Department of Biomedical Engineering

August 2005

APPROVAL PAGE

HAPTIC INDUCED MOTOR LEARNING AND THE EXTENSION OF ITS BENEFITS TO STROKE PATIENTS

Adrienne M. Coppa

Dr. Sergei Adamovich, Thesis Advisor — Date
Assistant Professor of Biomedical Engineering, NJIT

Dr. Richard Foulds, Committee Member — Date
Associate Professor of Biomedical Engineering, NJIT

Dr. Stanley Reisman, Committee Member — Date
Professor of Biomedical Engineering, NJIT

BIOGRAPHICAL SKETCH

Author: Adrienne M. Coppa

Degree: Master of Science

Date: May 2005

Undergraduate and Graduate Education:

- Master of Science in Biomedical Engineering,
  New Jersey Institute of Technology, Newark, NJ, 2005

- Bachelor of Science in Biomedical Engineering,
  Rutgers School of Engineering, Piscataway, NJ, 2003

Major: Biomedical Engineering

Publications:

Hung, G. K., Coppa, A. and Johnson, B. (July 2004). Aerodynamics and Biomechanics of the Free Throw. In G. K. Hung and J. Macari (Eds.), *Biomedical Engineering Principles in Sports* (pp. 367-390). New York: Kluwer Academic/Plenum Publishers.

To my Family, thank you for your unconditional love and support.

To my Mom and Dad, thank you for the opportunities you have given me.

ACKNOWLEDGMENT

I would like to express my gratitude to Dr. Sergei Adamovich, who served as my research supervisor. I would like to thank him for providing essential and frequent resources and insight. Special thanks are given to Dr. Richard Foulds and Dr. Stanley Reisman for participating in my committee.

Many of my fellow graduate students in the Biomedical Engineering Research Laboratories are deserving of recognition for their support, particularly Jean Kwon, Nelson Li, Amanda Irving, Satomi Suzuki, Kai Chen, and Kit August. I also wish to especially thank Qinyin Qiu for her continuous assistance and programming of the Haptic Master.

TABLE OF CONTENTS

TABLE OF CONTENTS
(Continued)

TABLE OF CONTENTS
(Continued)

LIST OF TABLES

LIST OF FIGURES

LIST OF FIGURES
(Continued)

CHAPTER 1

INTRODUCTION

1.1 Objective

The goal of this research is to determine an efficient method to induce motor learning in subjects with no history of musculoskeletal or neurological disorders through the use of virtual reality and haptics. Participating subjects complete different scenarios within a virtual environment and the learning evoked is measured through several parameters. The benefits to this study may then be transferred to stroke patients and other patients with musculoskeletal or neurological disorders, aiding in their motor rehabilitation.

1.2 Stroke: Causality and Incidence

Stroke is the primary cause of disability and the third principal cause of death in the United States. A stroke is a life-threatening event in which the brain does not receive enough oxygen. Loss of speech, memory, and motor skills are frequent complications associated with strokes. This study focuses on motor loss as caused by strokes and the rehabilitation from these losses. Many motor losses include paresis, loss of muscle control on one side of the body, facial droop, and temporary paralysis due to lack of motor control. Motor recovery following a stroke is frequently incomplete, therefore motor deficits remain a primary cause of long-term disability preceding a stroke. Recovery predictions can most accurately be determined by the initial severity of a stroke. Some stroke patients experience rapid improvement while others undergo

minimal improvement. Motor skill can be restored to a certain extent and the success rate of patients varies.

Rehabilitation treatments aimed at motor improvement for stroke patients are not fully understood. It is recognized that therapy, either constraint induced task training, or haptic treatments, almost always results in motor skill development. However, the mechanisms behind these developments need to be further comprehended to improve rehabilitation results. It is generally agreed upon that brain reorganization precedes motor improvement, but the mechanism behind brain reorganization is not entirely understood. It may be the result of a shift in activity from the ipsilateral to the contralateral side or it may originate from reorganization within specific brain regions, areas that are also disputed. In the future, gaining understanding of these current issues, motor rehabilitation techniques would greatly be enhanced, leaving many patients with vast motor skill improvements.

The clinical problem linked to strokes does not lie with the diagnosis of the occurrence, location, severity, or type of stroke. The issue is caused by the results of the stroke, mainly brain damage. In the United States, stroke is the primary source of disability. Only 10% of stroke survivors recover nearly completely, while a mere 25% recover with minor impairments. Forty percent of stroke patients experience moderate to severe impairments that require special care and 10% need care in a nursing home or long-term care facility. Fifteen percent of those who experience a stroke will die very shortly after. [1]

There are two types of strokes, cerebral ischemia and cerebral hemorrhage. Cerebral ischemia is induced by blockage in an artery that supplies blood to the brain and

causes a prolonged lack of oxygen rich blood to the brain. Cerebral hemorrhage results when there is bleeding of ruptured vessels into or around the brain. The risk factors associated with strokes differ between these two types. There are many risk factors that contribute to the occurrence of an ischemic stroke, but the most prominent one is age. People over the age of 65 are at an increased risk for an ischemic stroke compared to those in the younger population. High blood pressure and heart disease are also primary risk factors. The risk of a stroke occurring from these factors can be decreased through diet, exercise, and medication if necessary. Another high risk factor for ischemic strokes is atrial fibrillation, which occurs when muscles in the atria contract too quickly, resulting in an irregular heartbeat (arrhythmia). Arrhythmia alters blood flow and may cause blood clots to occur in the heart, which can then travel through blood vessels to the brain. A five-fold increase in the risk of a stroke is caused by atrial fibrillation. There are many other factors that heighten the risk of stroke occurrence. They include atherosclerosis (plaque build up in arteries), arterial stenosis (narrowing of arteries), cardiac conditions, fibromuscular dysplasia (causes stenosis and hypertension), and coagulopathy (blood-clotting disorder). Also included are alcohol or drug abuse (may cause decreased blood flow), smoking, infection (meningitis, endocarditis), high blood pressure or high cholesterol, brain tumor, and diabetes. Family/personal history of stroke, secondary hemorrhage following an ischemic stroke, sickle cell disease, a sudden rise in blood pressure, and surgical incision of an artery (treatment for atherosclerosis) also are factors that heighten the risk of an ischemic stroke. [2]

The risk factors concerning hemorrhagic strokes are fewer in number. They include an untreated aneurysm, congenital arteriovenous malformations, and traumatic

brain injury. Strokes develop more commonly under these factors and result when blood flow to a region of the brain is obstructed, giving rise to brain tissue death. [2]

The type of stroke and area of the brain that is affected alters the signs and symptoms that become apparent. Since strokes do not result in severe pain, patients often delay seeking treatment, which often causes repercussions furthering brain damage. Signs of an ischemic stroke appear suddenly and may only last a few minutes prior to subsiding. These symptoms require immediate attention to minimize the risk of brain tissue damage. Signs of a hemorrhagic stroke occur gradually. There are many symptoms that may occur prior to both types of strokes. They include difficulty speaking or understanding speech (aphasia), difficulty walking, dizziness or lightheadedness (vertigo), numbness, paralysis, weakness on one side of the body, seizure, severe headache, sudden confusion, sudden decrease in the level of consciousness, sudden loss of balance or coordination, sudden vision problems, and vomiting. [1]

Strokes have a vast impact on human performance. Depending on the area of the brain affected and the total brain cells killed, they can decrease or eliminate the ability to speak, use motor skills, and/or retain memories. The aspect that will be concentrated on in this research is motor loss. Rehabilitation methods, results, and imaging techniques regarding motor function are studied and compared.

Over 740,000 strokes occur in the United States each year, and approximately 150,000 of these result in fatalities due to either the short or long-term effects. Two-thirds of those who survive suffer from disabilities that range from moderate to severe. Over 30% of these survivors require assistance with daily living activities, another 15% need to be placed in an assisted living facility, and 20% of stroke victims require a cane

or walker to aid them in walking. Up to 33% of stroke survivors suffer from depression. There is almost two and a half (~ 2.4) times higher of a risk of stroke occurrence in African Americans than Caucasians and twice the risk of stroke in Hispanics than in Caucasians. Although males and females are equally likely to experience a stroke, females have a greater occurrence of death related to strokes. Ischemic stroke is more likely to occur in people over the age of 65 and hemorrhagic strokes are more common in younger people. [1, 2]

1.3 Physiology of Motor Behavior

Completing a coordinated movement is a complicated process that involves nerves, muscles, and bones. Motor units, which are comprised of one motor neuron and the skeletal-muscle fibers that the neuron innervates, are the building blocks for all movements. Motor neurons act as a final common pathway out of the central nervous system. [3]

The neurons involved in controlling motor neurons and skeletal muscles are organized in a hierarchical fashion, each level responsible for a specific task in motor control. The highest level of motor control forms complex plans in accordance with an individual's intention. Command neurons allow communication between the highest level and the middle level. The middle level then converts plans attained from the highest level to smaller motor programs, which establish the pattern of neural activation necessary to perform the movement. These programs are further broken down into subprograms that establish the movements required of individual joints. These programs and subprograms are then transmitted, via the cerebral cortex to the lowest control level,

or the local level. The lowest level indicates the tension of specific muscles and the angles of certain joints at the times necessary to complete the programs and subprograms received from the middle control level. [3]

The motor programs, which are patterns of neural activity required to carry out a chosen movement, are continuously adjusted throughout the course of most movements. While the initial motor program is being executed and the motion is underway, the middle level of the brain region is constantly receiving updated information regarding the motion taking place. Differences between the intended and actual movements are recognized, creating program adjustments that are sent via the local level to the motor neurons. When a complicated movement is frequently performed, the brain learns the program necessary to complete the action and the movement becomes a skill. Therefore, the information sent from the middle level is more accurate and requires fewer adjustments. However, less complicated movements that do not require fine motor skills are completed with only the initial motor program and at a higher speed. [3]

There are numerous motor centers in the brain that aid in influencing and controlling motor pathways. The sensorimotor cortex incorporates all regions of the cerebral cortex that work together to control muscle movement. The cerebral cortex aids in both planning and continuously controlling voluntary movements in the highest and middle levels of the motor control hierarchy. There are two primary regions of the sensorimotor cortex on the posterior area of the frontal lobe, the primary motor cortex and the premotor area. These two regions generate descending pathways for motor control. Movements of certain areas of the body are associated with particular regions of the primary motor cortex. The supplementary motor cortex, which is primarily located

on the surface of the frontal lobe, the somatosensory cortex, and the parietal-lobe association cortex are also involved in the control of muscle movement through the sensorimotor cortex. [3]

The various regions in the motor center of the brain are different both anatomically and functionally, but they are heavily interconnected with individual muscles and movements represented at multiple sites. The cortical neurons that control movement form a neural network; therefore many neurons participate in a single movement. A neuron functions in more than one movement. These neural networks that are formed are distributed across numerous regions, including the parietal and frontal cortex. The neural networks are flexible, and can therefore adapt to various circumstances. This adaptability allows neural signals from different sources to be integrated and result in an efficient movement. [3]

1.4 Introduction to Haptics

The study of haptics involves coupling the human sense of touch with a computer-generated virtual reality environment (VE). Haptics are used to increase the sense of presence or immersion in the VE, as the sense of touch is an important aspect of multisensorial communication. This allows the user a nonvisual means of recognizing that their hand is in contact with a virtual object. Haptics relate the ability to receive proprioceptive, tactile, and force feedback from the simulation in response to the user's actions.

There are two general fields of haptics, force (kinesthetic) feedback and tactile feedback. Force feedback concentrates on devices that interact with the muscles and

tendons. These devices allow the user the experience of the sensation of an applied force. Force feedback devices primarily are comprised of robotic devices that exert forces against the user, corresponding to the virtual environment and user's actions. Tactile feedback is the field of haptics that consists of devices that interact with nerve endings in the skin, to simulate heat, pressure, and texture. Tactile feedback devices have the ability to allow the user the knowledge of whether or not they are in contact with an object within the virtual world. Haptic tasks can also include tasks that involve the body's sense of propioception, which informs the user of their limb's positions relative to each other and the surrounding space. [4]

The addition of haptics to a virtual environment increases the amount of information that is processed by the brain. When developing haptic interfaces to be used by stroke patients and other people, the anatomy and physiology of the average user must be considered. Developing force feedback requires the average strength and size of joints, especially the hand, to be considered. When developing tactile feedback devices, factors of the human sense of touch must be considered. [4]

1.5 Haptic Master

Through the use of the Haptic Master it is possible to feel or touch a virtual object that has specific properties. This is achieved through incorporating force feedback and allowing three degrees of freedom. There are several principles of operation involved in the function of the Haptic Master. These include the control algorithm, the hardware, and the software.

The Haptic Master uses an admittance control algorithm, which means that the user exerts a force on the haptic device and the device reacts with the proper displacement. When the interaction force is measured, a virtual model calculates the position, velocity, and acceleration (PVA) that an object in space would receive as a result of this force. The space an object exists in (including gravity, environmental friction, etc.) and the object's properties (mass, damping, friction, stiffness, etc.) are defined by the virtual model. In order to avoid infinite accelerations and system instabilities, the virtual model usually contains a mass larger than zero. The PVA-vector acts as a reference signal for the robot, and a high bandwidth PID (proportional integral and derivative position loop) servo control loop controls the robot to the specified PVA vector. The proper feedback gain settings allow the control loop to cancel the actual mass of the manipulator to a factor of six and to also cancel the internal friction up to the accuracy of the force sensor. [5]

The Haptic Master hardware contains two primary parts, the robot arm and the control unit. The robot arm acts as the force display and the control unit contains the electronics, including safety relay, amplifiers, and the haptic server. The robot arm is built to allow for zero backlash and minimal weight. This is important because the human sense is very sensitive to vibration effects and the human tactile senses can have a spatial resolution as high as ten to 100 microns for vibration. Also, a low weight is necessary for safety aspects. The kinematic chain from the bottom up generates base rotation, up/down arm movement, and in/out arm movement, which allows for three degrees of freedom at the end effector. Various end effectors can be attached to the force sensor to complement the application. For example, tools can be attached to an end

effector and the tool contact forces can be simulated in a virtual setting. Or, it is possible to use an end effector that the patient's arm can be placed in, which would allow for increased degrees of freedom and could treat stroke patients undergoing rehabilitation therapy. [5]

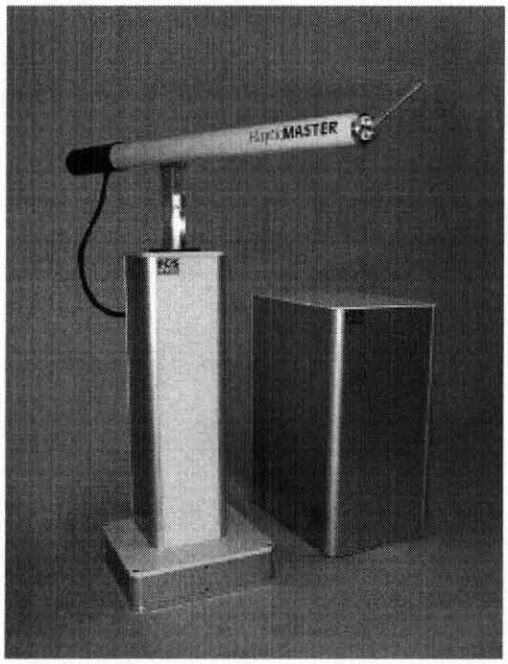

Figure 1.1 A picture of the Haptic Master system. The control unit (right) encases the necessary electronics (amplifiers, safety relays, and haptic server) and the robot arm (left) is the force display.

Source: R. Q. van der Linde and P. Lammertse. [5]

The control unit contains various electronics. The virtual model is executed by a PC with a VxWorks real-time operating system, called the haptic server. This system runs at a fixed rate of 2,500 Hz refresh rate. This frequency permits a haptic quality that is a smooth and realistic experience because it is approximately ten times greater than the maximal human discrepancy value. The PID control loop operates on the amplifiers at a rate of 20 kHz pulse width modulated frequency, which works by switching the power

supply on and off very rapidly. If the switching frequency is high enough, the motor runs at a steady speed. [5]

The user can create a virtual model on the haptic server through the use of an application programming interface (API). The haptic server is able to translate the virtual model and create the trajectories for the robot based on the force sensor input. It takes into account factors such as safety guards, communication protocols, and collision detection with virtual objects. The API makes an Ethernet connection to the Haptic Master in order to control and modify the virtual haptic world and the internal state machine. Haptic effects, such as springs and dampers, can be incorporated into the environment and spatial geometric primitives, such as spheres, cones, and cubes, can be defined. Combining these functions allows simple, virtual worlds to be created. More complex virtual worlds can also be constructed through the use of other rendering methods. A local mass model will be received on the haptic server. The forces acting on this mass resulting from interaction with the virtual world are received from the host PC. [5] Programming the Haptic Master allows various properties to be specified for objects. Several programs can be used to control the Haptic Master, including Matlab, which is translated through the interface Maptic, from Matlab to the Haptic Master. C^{++} and Open GL can also be used to directly program the Haptic Master. The general specifications of the Haptic Master are shown in tables 1.1 and 1.2.

Table 1.1 Haptic Master General Specifications

Specifications	Value
Workspace volume	80 (l)
Position resolution at end effector (no load)	4-12 (μm)
Mechanical stiffness at end effector[a]	
X-direction	400 (N/mm)
Y-direction	07 (N/mm)
Z-direction	41 (N/mm)
Nominal/peak force	100/250 (N)
Minimum tip inertia	2 (kg)
Maximum velocity at end effector (no load)	1.6 (m/s)
Maximum acceleration/deceleration	10/50 (m/s^2)
Force sensitivity	0.01 (N)

Note: [a]At 1 kg load, in the middle of the workspace

Source: R. Q. van der Linde and P. Lammertse. [5]

Table 1.2 Force Controlled Devices on Haptic Performance Indicators Comparison

	Haptic indicators			
Robot name and type	Haptic resolution × 10^{12}	Force depth	Inertial ratio × 10^3	Remark
FCS HapticMaster	710	1×10^4	14-25	
Epson EL850	190	1×10^4	–	Industrial robot
Stäubli RX90b	370	1×10^4	–	Industrial robot
Mitsubishi electric RV-3AJ	26	1×10^4	–	Industrial robot
WAM arm	0.13	23	–	Impedance mode
Phantom desktop	0.38	28	42	Impedance control
Phantom Premium 3.0	25	15	6.7	Impedance control
Delta HD 3DOF	0.02	15	125[a]	Impedance control

Note: [a]Estimated value

Source: R. Q. van der Linde and P. Lammertse. [5]

1.6 OpenGL Programming

The programming of virtual environments used in this research is done with OpenGL. OpenGL is one of the primary programs for creating portable, interactive 2D and 3D graphics applications. OpenGL incorporates a wide set of rendering, texture mapping,

special effects, and other powerful visualization functions, which aid in increasing the development and advancement of its applications. [7]

There are several advantages to using OpenGL. OpenGL is the only truly open, vendor-neutral, multiplatform graphics standard. It is a stable program that avoids producing additions that cause the existing applications to become obsolete. OpenGL applications produce consistent visual display results on any OpenGL API-compliant hardware, regardless of the operating system. New hardware innovations are accessible through the API via the OpenGL extension mechanism, which allows application developers and hardware vendors to incorporate new features into their normal product release cycles. OpenGL can run on a wide variety of systems, including PCs, workstations, and supercomputers. OpenGL is a fairly easy program to use, with an intuitive design and applications that generally require fewer lines of code than other programs. [7]

OpenGL programming simplifies the development of graphics software and gives software developers access to geometric and image primitives, display lists, modeling transformations, lighting and texture, anti-aliasing, blending, and other features. OpenGL standards have language bindings for C, C++, Fortran, Ada, and Java. Applications that use OpenGL functions are easily portable across a wide array of platforms for maximized programmer productivity and shorter time-to-market. OpenGL supports visualization applications with 2D images that are treated as types of primitives, which can be maneuvered similar to 3D geometric objects. [7]

OpenGL is continuously being developed, with formal revisions occurring at periodic intervals. Extensions that allow application developers to utilize the latest

hardware advances through OpenGL are constantly evolving. When extensions become broadly accepted, they are considered for addition into the main OpenGL standard, therefore OpenGL advances in a controlled and innovative manner. [7]

1.7 Matlab

The analysis of collected data in this study is completed with Matlab. Matlab is a high-level technical computing language and an interactive environment for algorithm development, data visualization, data analysis, and numerical computation. Matlab allows the user to compute technical problems faster than more conventional programming languages, such as C, C++, and Fortran. There is a wide range of applications for Matlab, which include signal and image processing, communications, control design, test and measurement, financial modeling, and analysis, and computational biology. Particular classes of problems can be solved through add-on toolboxes available separately. There are several key features to Matlab, including high-level language for technical computing, development environment for managing code, files, and data, interactive tools for iterative exploration, design, and problem solving, mathematical functions for linear algebra, statistics, Fourier analysis, filtering, optimization, and numerical integration, 2D and 3D graphics functions for visualizing data, tools for building custom graphical user interfaces, and functions for integrating Matlab based algorithms with external applications and languages, such as C, C++, Fortran, Java, COM, and Microsoft Excel. [8]

Matlab supports the vector and matrix operations that are essential to engineering and scientific problems. The Matlab language enables fast development and execution.

It allows the programming and development of algorithms to be completed faster than with customary languages by avoiding having to perform low-level administrative tasks, such as declaring variables, specifying data types, and allocating memory. Often, MATLAB eliminates the need for 'for' loops. Therefore, one line of MATLAB code often replaces several lines of C or C++ code. However, Matlab still provides the features of a traditional programming language, such as arithmetic operators, flow control, data structures, data types, object-oriented programming (OOP), and debugging features. [8]

1.8 Other Rehabilitative Devices Used

1.8.1 MIT-Manus

There are several requirements in developing force feedback devices. They need to be powerful, in order to actively oppose the user's motion. However, they also need to be light and un-intrusive to avoid the user's fatigue. Force feedback devices must be able to maintain forces for a long period of time without overheating. They have to be safe and clean for the user. Force feedback devices may be portable or nonportable. Nonportable devices are attached to a desk, floor, or wall and may be heavier than portable devices. [9]

The MIT-Manus is a two-degree-of-freedom robot manipulator that uses two PCs for control and visual/auditory/force feedback to the patient. The MIT-Manus, which is derived from the Latin "mens et manus" (mind and hand), was created at Massachusetts Institute of Technology (MIT) and has been undergoing development for approximately 15 years. This robot is attached to the patient's lower arm and wrist with a brace,

allowing both translations in a horizontal plane and rotation of the wrist. A video screen signals the beginning of the treatment by instructing the patient to complete an arm exercise, such as connecting the dots. If the patient begins the arm movement on their own, the MIT-Manus guides the movement with variable levels of assistance. However, if the person is unable to begin the motion independently, the robot moves their arm through the exercise. [9, 10]

1.8.2 Rutgers Master II ND Glove

The RMII Glove (Rutgers Master II ND) is a compact haptic interface created at Rutgers University. Another similar apparatus, the CyberGlove from Immersion Co., is used in related studies. The RMII Glove uses custom pneumatic actuators, located on the thumb, index, middle, and ring fingers, to resist finger motion. It allows four degrees of freedom for each finger and can be adapted to different finger sizes. The glove is very light, powerful, and is capable of maintaining high forces to each finger without overheating. This allows the user the same opposing force that occurs when an object in hand is squeezed and opposes the force created. Therefore, the glove can create a force applied by a virtual object on the hand with the same intensity and direction as an actual object. [11]

The device applies a torque equal to that of the interphalangian joint to the user's fingertips and uses noncontact position sensors to measure the fingertip position with respect to the palm. Each finger actuator can apply up to 16 N of force when pressurized at 100 psi. The air pressure is produced by a portable air compressor. Infrared sensors located inside the actuators measure the displacement of the fingertip in relation to the

exoskeleton base attached to the palm. Hall-Effect sensors at the base of the actuators determine their flexion and abduction angles with respect to the base. The RMII glove is connected to an electronic Control Interface that reads the RMII sensors, controls the desired fingertip forces, and calculates the joint angles. [9]

The RMII glove is calibrated by reading the sensors when the hand is completely opened. The values are read at the maximum piston displacement, maximum flexion angle, and the neutral abduction angle. The control interface controls the actuator forces at a rate of 300 Hz, through a servo loop implemented in software on a Pentium 233 MHz embedded board. [9]

Interfacing the RMII glove with a PC allows the running of both the virtual reality simulation exercises and a database. Performing local computations on the embedded Pentium frees the host PC to perform mostly graphics computations at high enough frame rates, which are required for VR simulations. The host PC and the electronic interface communicate through a serial line at a rate of 38,400 baud. This rate allows the host to receive 157 datasets (hand configurations) every second. [11, 9]

1.8.3 Rutgers Ankle

The Rutgers Ankle interface allows the control of forces and torques throughout the full range of motion of the foot in six degrees of freedom. Linear potentiometers, which function as position sensors, are attached in parallel with each cylinder. The force, torque, position, and orientation at the patient's foot are measured by a six-degree-of-freedom force sensor between the mobile platform and foot restraint. The platform is connected to an electro-pneumatic controller, which regulates the air pressure in the

platform actuators using solenoid valves. The controller also holds amplifier boards, A/D/A boards, and an embedded 233 MHz Pentium Board operating Windows 95. This computer maintains the actuator servo control by offloading the corresponding computations from a host computer. The Rutgers Ankle is a Stewart-platform type haptic interface that uses double-acting pneumatic actuators, with high power/weight ratio and extremely low friction, which allows for small overall dimensions and low weight. [9]

1.8.4 PHANToM

The PHANTOM line of haptic devices is produced by SensAble Technologies. They allow for users to touch and manipulate virtual objects. There are various models of the PHANTOM, which make it possible to meet the needs of research and commercial customers. The PHANTOM Premium models are high-precision instruments and provide the largest workspaces and highest forces. Some of these models offer six degrees of freedom capabilities. The PHANTOM Desktop Device and the PHANTOM Omni device are more affordable desktop solutions. The PHANTOM Desktop supplies high fidelity, strong forces, and low friction, while the PHANTOM Omni is the most cost-effective haptic device currently available. [12]

1.8.5 Stereographics CrystalEyes Workstation

CrystalEyes is a set of liquid crystal shutter eyewear for Stereo3D imaging in scientific and engineering applications. They are lightweight and wireless. They allow high-definition, stereoscopic 3D images on major UNIX platforms and Windows 2000/NT/XP in CAVEs, theaters, and immersive environments when used in conjunction with

compatible software and standard workstation displays. A CAVE is a room-sized, virtual reality theater where computer images are rear projected onto the walls and front projected onto the floor. Within a CAVE system, the user's position relative to the virtual environment is tracked by sensors. CrystalEyes is triggered by an infrared emitter that is connected to the user's workstation. CrystalEyes is the leader in 3D visualization for virtual prototyping, molecular modeling, and serial photography/mapping. The industry criterion for scientists and engineers who develop, analyze, and employ 3D computer graphics in CAVEs, theaters, and immersive environments is founded by CrystalEyes. [6]

1.9 Other Programming Languages Used

Many of the virtual reality programs developed and used in these studies were created using WorldToolKit, which is a cross-platform software development system for building high-performance, real-time, integrated 3D applications for scientific or commercial use. The use of this high-level application programming interface (API) allows for the rapid development of prototypes and reconfigurations of an application. WorldToolKit also has a function library and end-user productivity tools that are necessary in developing applications. It has the capability of supporting network-based distributed simulations, CAVE-like immersive display options, and the industry's biggest display of interface devices. [13]

CHAPTER 2

LITERATURE REVIEW

2.1 Robotics and Rehabilitation

Every year approximately four million United States citizens suffer from the effects of strokes, leaving patients requiring therapy for difficulties with language, memory, or movement. The use of robotics aims to treat motor problems through encouraging and challenging patients to participate in therapy. Task oriented repetitive movements can be used as physical therapy treatment to improve the muscular strength and coordination of patients with impairments due to neurological lesions. [14]

Several institutions have produced robots that work in conjunction with physical therapists to help patients reduce their level of motor disability and become more independent. These robots have been created to assist patients in continuously exercising an arm that has been paralyzed by a stroke, regardless of whether the patient is able to move their arm independently. The MIT-Manus, which is described in the previous chapter, is one of the most well-known and widely used devices in this field. [10]

In a three-year clinical trial, published May 23, 2000 in *Neurology*, two groups of stroke patients received standard daily physical therapy. The experimental group underwent a daily additional hour of robot therapy using the MIT-Manus while the control group received an extra hour of sham therapy. The sham therapy consisted of using the robot, but it did not aid in guiding the patient's arm. The patient was to use their unaffected arm as a guide in completing the exercises. The results of this study showed that the experimental group had twice the motor advancement as the control

group. Many movements, such as reaching, sweeping, and support, which involve the upper arm and shoulder, were improved. The control groups therefore achieved increased arm functionality during everyday tasks, such as grooming oneself. [10]

Another study was designed to examine whether robotic therapy could reduce motor impairment and increase the recovery of the affected arm in patients with chronic stroke. The patients involved in this study included 20 people (16 men, four women) who had an incident of a single, unilateral stroke within the past one to five years. They all experienced persistent hemiparesis. The patients had adequate cognitive and language abilities to allow them to understand and follow instructions. [15]

Baseline clinical evaluations were performed to establish motor stability of the affected upper limb at two-week intervals during a one-month observation period prior to robotic therapy. The Modified Ashworth Scale, the Fugl-Meyer test, and the MRC test of Motor Power were used to measure muscle spasticity, upper-extremity function, and motor power. The Motor Status Scale (MSS) score allowed for an inclusive and discrete analysis of upper limb movement and function. [15]

Robotic therapy, using the MIT-MANUS, was completed three times a week for an hour over the course of six weeks. The therapy consisted of goal-directed, planar reaching tasks to exercise the hemiparetic shoulder and elbow. Subjects participated in either the sensorimotor group or the progressive-resistive therapy group, depending on the patient's motor ability of the involved limb. In the sensorimotor group, the robot assisted the patient when they were unable to reach targets independently. After three weeks of therapy, if subjects were able to independently reach all targets they were randomly assigned to either continue in the sensorimotor group or switch to the

progressive-resistive therapy group. In the progressive-resistive group, the patients performed the same goal directed, planar reaching tasks. However, they were also moving against an opposing force generated by the robot. The degree of this force was established through an algorithm that used robotic measures of the patient's muscle strength to adjust the efforts required to reach the targets. [15]

The results of this study showed statistically noteworthy improvements from admission to discharge on the Fugl-Meyer test, MSS score, and the motor power score. A secondary examination demonstrated differences between the two groups. Those in the progressive-resistive therapy group underwent nonspecific improvements on the wrist and hand MSS scores that were not seen in the sensorimotor group. These results demonstrate that robotic therapy has the potential to work well with other treatment methods through reducing motor impairments in patients with moderate to severe chronic impairments. [15]

The MIT-Manus has successfully treated patients who experienced a stroke one to five years previous to its use in therapy, which is well beyond the generally accepted recovery time frame of three months post stroke. However, the level of neuro-recovery, and therefore motor rehabilitation, is highly dependent on stroke location. [14]

Despite the benefits to the MIT-Manus, there are several drawbacks. Due to the cost of the robot, which is approximately $70,000, patients are not yet able to own or rent the robot for home use. Having this accessibility to the MIT-Manus would allow for even greater rehabilitation levels in patients. Also, the MIT-Manus can only aid in increasing shoulder and elbow movements in patients. For patients to obtain the highest level of motor improvement from robotic rehabilitation, it is necessary to use their hands.

However, there are alternative means of improving hand movement, such as constraint-induced therapy or the use of other robots. [16]

2.2 Robotics, Haptics, and Rehabilitation

Haptics have been incorporated into many therapies used to treat motor disabilities caused by strokes, muscular dystrophy, and spinal injuries. There are several variations of haptics that have been used in treatments for hand rehabilitation. A mouse-based force-feedback device is inexpensive and capable of forming haptic interactions with the user due to its wide variety of movement generation capabilities. The force feedback within this device consists of constant directional forces, tactual, and vibration sensations that correspond with the user interface. [17]

Experiments were designed in Cambridge, UK that studied the effectiveness of treatment with a force feedback mouse. Force feedback within the mouse was able to produce constant directional forces and tactual and vibration sensations corresponding to user interface events. The first two week experiment involved four motion-impaired users, two who were severely impaired by tremor, weakness, and spasm and two who were only slightly impaired. In this study, a 2D projection of a map of the United States was displayed and ten cities were marked as target locations. A start signal was displayed at a particular city and the patient was to move to and click on the inner circle of the targeted city. When force feedback was incorporated into the experiment, the mouse was strongly attracted to the center of the target once the outer circle of the target was reached. Without the use of force feedback, the user interface acted as a normal

point and click mouse. This experiment was performed at different levels, with varying target sizes. [17]

Although the results of these experiments varied amongst the participants, there was significant improvement in the time necessary to complete the tasks and the error rate that occurred with the use of force-feedback. A considerable amount of learning was seen to occur from task to task amongst the patients and the times to complete the first task were reduced by 30 to 50% when the task was completed with force-feedback assistance. The results from one user showed they were unable to perform the task at the easiest level of the unassisted mode and took up to 364 seconds to complete half the targets. With the force-feedback assistance, they were able to complete five trials and displayed significant learning over several trials. The scores of all the users were improved while using the force-feedback system. Approximately half the time was required to complete the tasks with assistance from the force-feedback system. [17]

A second study was conducted using the same force-feedback mouse. Sixteen target circles were displayed equidistantly around a central circle. The patients were to click the target circles in a random order determined by the computer program. When the cursor grew near each target circle it was attracted from the outer region of the circle towards the circle's center. The impacts of several variables were analyzed during this study, including pointer trails, vibration, target color change, force feedback, and time to complete a selection. [17]

The results of this study show that the attraction from the outer region of the circle to its center decreases the time to complete the task by 10 to 20%. The more severely impaired users benefited more from the use of the attraction to the center of the

circle. Among the variables incorporated into this experiment, force-feedback was seen to be the most beneficial. Through the use of cursor traces, it can be seen that force-feedback greatly aided the users in completing the task. The addition of vibration to the mouse almost doubled the time required to perform the task for all of the users. [17]

A force feedback glove, the Rutgers Master II-ND Glove, is another haptic device that is used for hand rehabilitation. This device is described in the previous chapter. Several studies have been conducted using the Rutgers Master II-ND Glove or a similar apparatus, called the CyberGlove from Immersion Co. Through the use of these two devices, finger range of motion, finger flexion speed, independence of finger motion, and finger strength can be exercised.

One study that was conducted through NJIT, UMDNJ, and Rutgers University involved eight post-stroke subjects. The aim of this study was to determine the degree to which motor skills acquired through virtual reality haptic training could be successfully applied to real world arm and hand movements in the post stroke subjects. The eight subjects included in the study participated in almost three weeks of training, which consisted of 13 days of training and two weekend breaks. Four hand exercise simulations in the form of simple games that were developed using WorldToolKit graphics library were used during the training. Auditory, visual, and numeric feedback regarding their performance was given to the subjects. The training sessions consisted of four training blocks, range of motion, speed of movement, fractionation of individual finger motion, and strengthening of the fingers. [18]

The analysis of the transfer of the improvements achieved through virtual reality therapy to real world situations was tested through several tests. The Jebsen Test of Hand

Function, which includes tasks such as writing, turning index cards, picking up small common objects, simulated feeding, stacking checkers, picking up large light objects, and picking up large heavy objects, was used to test hand function during real world activities. The kinematics of finger and arm motion during these tasks was analyzed. Also noted were the 3D coordinates of the arm joints and trunk. This was achieved through the use of electromagnetic position sensors (Flock of Birds, Ascension Technologies Inc.). The finger joint flexion and extension were attained from resistive bend sensors in the CyberGlove. Also included in the analysis were the flexion/extension of the metacarphophalangial (MCP) and proximal interphalangial (PIP) joints of the five fingers, the abduction/adduction joints of the index-middle and middle-ring fingers (ABD), and the thumb rotation and abduction. [18]

The results of this study show that six of the eight subjects increased their finger and thumb range of motion. Four subjects notably improved their finger speed and two subjects their thumb speed. Seven subjects improved their fractionation and three improved their finger strength. Also, one week following the study, patients showed good retention of this progress. These improvements were shown to carry over to real life arm movements through the Jebsen Test of Hand Function. There was a reduction of time necessary to complete a task with the affected hand. Improvements in certain aspects of hand kinematics during grasping were seen; there were less abnormal finger flexion-extension patterns and increased variability and desynchronization between the hand and finger motion. The time from hand peak velocity to the moment when the object was lifted from the table decreased significantly after the treatment, showing an average of 22% faster task completion. However, the time to peak velocity and the peak

velocity of the affected hand was not improved by the treatment. This result was somewhat expected due to the lack of elbow and shoulder therapy during the training. [18]

Another study demonstrates the benefits of computerized training in a virtual reality environment to retraining the hand of stroke patients who are in the late recovery phase. This investigation included three subjects who were all right-handed with a left hemispheric stroke that had occurred within the past three to six years. The subjects were currently not receiving any therapy for their rehabilitation. All of the patients had the ability to extend the wrist of the hemiplegic limb 20 degrees and the metacarpophalangeal joints at least 10 degrees. The subjects were an 83-year-old woman (ML), a 54-year-old man (LE), and a 59-year-old man (DK). [19]

Prior to and following the two-week training period, patients were evaluated with the Jebsen Test of Hand Function and seven items from the hand division of the Fugl-Meyer Assessment of the Sensorimotor Recovery After Stroke. The 3.5-hour daily training consisted of a virtual reality exercise system that displayed 3D graphics on a flat computer screen and two hand devices, the CyberGlove and the Rutgers Master II-ND. The CyberGlove aided in developing the range of motion, speed, and fractionation movement exercises. The Rutgers Master II-ND was beneficial in finger strengthening. The patients received haptic, visual, and auditory feedback while completing four different exercises in the form of computer games that were designed using WorldToolKit. Each exercise was designed to focus on the development of various hand motions, such as range of motion, speed of movement, fractionation of individual finger motion, and strengthening of the fingers. For the nine days that the therapy period

required training, the goal was to complete four VR training sessions a day. Subject ML completed 35 training sessions in the two-week period, LE completed 31 sessions, and DK 32 sessions. [19]

Subject ML improved the range of motion and speed of movement in her thumb and fingers throughout the training. The functionality of her hand was shown to have increased by the Jebsen Test of Hand Function. She reported improvements in her everyday life, such as eating and moving the lever on her recliner chair, as a result from the therapy. Subject LE showed improvement in the fractionation and range of motion of his thumb and fingers. There were improvements in the computer measures of his hand function, however no improvements in the Jebsen Test of Hand Function were seen and he did not report any improvements in his hand function at home. Improvements in the range of motion and strength of the thumb, velocity of the thumb and fingers, and fractionation were seen in DK's performance. Subject DK was seen to have the highest functioning hand level amongst the three patients following the therapy; however, his affected hand was functioning at higher levels prior to the treatment. After the therapy, he reported being able to use his right hand in assisting steering his car, buttoning his shirt, and was practicing using his affected hand with the mouse. Following the therapy, the patients reported that they believed continued VR therapy would further improve their hand function. [19]

The Rutgers Ankle Haptic Interface is another virtual reality system used to aid in rehabilitation, which is discussed in the previous chapter. The Rutgers Ankle measures foot position and orientation, while providing resistive forces and torques through a computer-controlled, compact, robotic platform. Research was conducted to analyze the

degree to which patients benefited from the inclusion of the Rutgers Ankle in their rehabilitation therapy and to determine how well the Rutgers Ankle functioned in a clinical setting. In this report, three case studies were conducted. Each of the three subjects participated in two-week trials using the Rutgers Ankle in addition to their regular rehabilitation program. [20]

The first day of the study included a clinical exam where each of the subjects was tested on ankle strength, range of motion, balance, and functional ability measures. They were also instructed on and practiced on the Rutgers Ankle and performed a baseline test, which measured displacement and torque for ankle motions. The subjects completed a subjective questionnaire to rate their experience learning and utilizing the Rutgers Ankle and virtual reality interface. Following the initial day, every other weekday, subjects exercised on the virtual reality system for 30 minutes, which consisted in total of five sessions. The virtual reality video game consisted of an airplane that was to be flown at various speeds through a certain number of hoops located in numerous positions. Training was customized for each of the three subjects and their progression. A sixth session was included for the patients to complete a clinical exam using the Rutgers Ankle and another subjective questionnaire. [20]

The first patient was a 14-year-old male with a Grade I inversion sprain that resulted from wrestling. His therapy with the Rutgers Ankle began two weeks following his injury. He quickly mastered the virtual reality simulation, as he had a great deal of exposure to computer games. He progressed to the most difficult level of training at the highest level of resistance. His overall accuracy improved from 36 to 42% for pitch, 37% for roll, 38% for combination movements, and 100% for all movements at a comparable

level of speed, difficulty, and resistance. Following the treatment, he was able to maintain his balance for a longer period of time and could ascend and descend stairs faster without experiencing pain. After the therapy, this patient was able to return to wrestling. [20]

The second patient was a 15-year-old female with a Grade II inversion sprain that resulted from softball. The sprain occurred five months prior to this study. Unlike the previous patient, she had no previous experience with video games. She progressed from the second to the third level of resistance and from the easy to the medium level of difficulty, with only a few trials at the most difficult level. The therapy resulted in pain in her ankle and aggravation of her symptoms. Frequently, ice packs were applied to her ankle after the simulations. However, at the end of training, there were improvements in her strength and balance. Her accuracy increased from 56% for pitch, 67% for roll, and 65% for combination movement, and 100% for all movements. Also improved were her dorsiflexion plantarflexion, dorsiflexor and everter peak ranges of motion, and her dorsiflexor, everter, and plantarflexor torques. After the therapy, she continued to play softball. [20]

The third patient was a 56-year-old female with a bi-malleolar fracture. The fracture was reduced with an external fixator two months prior. Therapy began at very low speeds on the easiest range of motion setting. By the last session she was testing at slightly higher speeds and at the medium range of motion setting. Improvements in her ankle's range of motion, balance, strength, and speed were seen as a result of the combined therapy. The Rutgers Ankle allowed her improvements in the range of motion of ankle everters and plantarflexors. The amount of torque she produced also increased

for ankle everters and dorsiflexion. During the training period, the patient was able to return to hiking. [20]

These studies show the ability of the Rutgers Ankle to be used as an effective rehabilitation therapy. This is the first clinical data to be collected using the device in conjunction with virtual reality simulations. The ability of haptic therapy used in conjunction with virtual reality to aid in the physical rehabilitation of patients in areas of the body other than the hand and arm is shown through this study.

Another study completed incorporated the use of multiple rehabilitation devices, the Rutgers Masters II Glove and the Rutgers Ankle. The purpose of this study is to depict the development and testing of two haptic devices designed especially for rehabilitation in a virtual environment. Their effectiveness in strength and functional training of the hand and the lower extremity of patients post-stroke is shown. In this study two patients are treated. [9]

The first patient (EM) was a 73-year-old left-hand dominant male who experienced a right cerebral vascular accident two years before participating in the study. He is independent in his self-care activities including movement on level surfaces and stairs using a cane. [9]

During the training, clinical and VR measurements were taken using the RMII glove. Mean grip force was measured at three intervals using a dynamometer. Functional changes were used to measure the Jebsen Test of Hand Function, which included seven fine motor activities. [9]

The training took place in a laboratory setting and lasted three weeks, with 13 days of training and weekend breaks. There were pre- and post-tests. Each virtual reality

exercise session included four training blocks; range of motion, speed of movement, fractionation of individual finger motion, and strengthening of the fingers for a total of 130 trials for each session. Each day there were four to five sessions of VR exercise, which lasted two to two and a half hours daily. Strengthening exercises involved wearing the RMII glove, which applied forces to his thumb or index, middle, and ring fingers. The graphical interface displayed an image of the RMII glove and EM was to push down each piston with either his thumb or three fingers against a predetermined force. Subject EM had to move 80% of his initial range of motion against the glove's resistive force. [9]

The results of this study showed improvements in EM's hand function. Three dynamometer readings were taken before, during, and after the 13 training sessions and showed that the grip force in his left hand increased from 8.6 kg to 17.3 kg from the beginning to the end of the study. The grip force in his right hand (unaffected) was only slightly increased throughout the study, from 40 kg to 41.3 kg. These improvements indicate an improved ability to produce work. The Jebsen Test of Hand Function demonstrated a small decrease in time required to pick up heavy objects. A questionnaire given at the end of the study indicated that EM felt the training had a positive impact on his hand function and he felt that further improvements might have occurred if the training had continued. He also said that he had wished the training had been part of his original therapy. [9]

The second patient (JB) was a 70-year-old right-hand dominant male who suffered a right ischemic middle cerebral artery stroke 11 months prior to the treatment.

He was able to walk short distances (one block) with a quad cane and ascend four steps. He fatigued easily and often "caught his foot" while walking. [9]

On the first day of the study, clinical and virtual reality baseline tests were conducted. Clinical tests involved lower extremity range of motion, sensation, strength measurements, balance, and skin condition. The virtual reality testing included movements with the Rutgers Ankle through the maximum range of motion and maximum torques for the dorsiflexion/plantarflexion and eversion/inversion. Also measured in the VR training were target accuracy, number of hoops that were either entered or hit divided by the total number of hoops in the simulation, and total training time during each session. [9]

The VR training lasted two weeks, and each individual training run lasted from two to five minutes. Subject JB was to perform movements of dorsiflexion/plantarflexion and eversion/inversion with his ankle, as well as combined movements to move the plane through targets. He had greater difficulty with inversion/eversion; therefore these movements were completed at a slower speed with a larger distance between the targets. The training did not include any task specific activities, such as walking or climbing stairs. Unlike EM, JB's training was conducted in an outpatient clinic where other patients were either being treated on plinths or were supervised while they exercised. [9]

The results of this study show that JB experienced a one grade increase in strength for his involved lower extremity for inversion and eversion (4/5 to 5/5). His strength for dorsiflexion was 5/5 and plantarflexion was not measured. There was an increase of 10 degrees for his range of motion for plantarflexion (to 45 degrees) and a 5 degrees

increase for dorsiflexion (to 5 degrees). Torque was increased for all trained motions on the involved side and for plantarflexion on the unaffected side. His accuracy improved for all motions; from 32 to 95% for pitch, from 84 to 93% for roll, and from 58 to 88% for the combined motion. Overall, JB felt that he was now 55% recovered from his stroke. He increased his walking distances and now uses a single point cane rather than a quad cane. He reported that he found the simulation easy to understand and enjoyable. Following this training, JB completed an upper level extremity virtual reality-training program and became interested in returning to playing golf, despite some difficulty in gripping the club with his left hand. [9]

Both patients involved in this study demonstrated improvements in the strength and function of their affected extremities. The resistance and force feedback used in the training with the RMII glove and the Rutgers Ankle allow for an expected increase in strength. Because the length of the training was only 2 to 3 weeks, the strength improvements are attributed to neural rather than hypertrophic changes. The subjects both showed improvements in function in the absence of task specific training, which suggests that there may be a relationship between strength gains and functional improvements. The flexibility of the VR tools described in this paper is supported by the differences between the two patients' capabilities and the manner and location in which they were trained. [9]

A single case study was completed to determine if training in a virtual environment with a haptic device would improve the motor function in the left hemiparetic arm of a stroke subject. The haptic device used in this study is the PHANToM. [21]

The patient participating in this study was a right-handed man in his late 50s who experienced a first occurrence stroke in the right genus of the internal capsule. It had been 12 weeks since the stroke when treatment began. The man was able to ambulate independently and could partially move his arm with some wrist extension. He had a weak lateral grasp, but had no limitations in finger extension and flexion. The patient completed most of his activities of daily living (ADLs) through compensation with his right arm. [21]

Training took place in a university hospital's laboratory. It consisted of an initial baseline session, an intervention phase, and a follow-up phase where three tests and an interview were conducted to determine motor performance. The Purdue pegboard test was the first analysis conducted. It evaluated unilateral and bilateral dexterity for two types of activity; gross movements of hands, fingers, and arms, and finger dexterity. This test had two subtests, the first which tested the ability to place as many pegs as possible with the left hand into the holes on the left side of the board and the second which tested the capacity to place as many pegs as possible into the board using both hands. The dynamometer hand-grip strength was measured in the second test. The peak maximum grip force and the mean value of the ten second sustained grip were recorded. [21]

A third test was an upper-extremity test, in which a haptic device (the PHANToM) was moved to different targets on the screen. The motions required were in different directions, sideways, up, down, and diagonal. The time, speed, trajectory distance (actual pathway of the upper extremity), and the intertarget distance (actual pathway of the upper extremity) were measured to assess the performance. As a reference, nine healthy men, all right-handed, and with a mean age of 50 years completed

the same test as the patient. An interview was conducted to learn about the use of the affected upper extremity in ADLs at home. [21]

The third, haptic test used a programming environment, Reachin API, which allows for interactive manipulation of a 3D model by using a haptic interface. The patient receives translational, rotational, and torque feedback from the PHANToM device. They wear special stereo viewing glasses, called Crystal Eyes, which allow them to view 3D objects. The training consists of a computer game, 3D bricks, that begins when the subject strikes a ball and then begins to try and knock bricks down. Points are given for bricks that are knocked over, and negative points are given when the subject misses the ball. The game can be played at four levels, where the velocity of the ball is increased with increasing levels. [21]

The results of this study show improvement of the affected limb. Fine manual dexterity was shown to improve by 11% units after the intervention and continued to improve to 17% units at follow-up. The mean grip force at baseline was 13% of grip force and increased to 57% at follow up. The median intertarget time to complete the virtual reality test decreased from 1.27 to 0.96 seconds post training and further decreased to 0.86 seconds during follow-up. The trajectory distance and the intertarget distance did not indicate any major changes after the intervention period and during follow up. In a follow-up interview, the subject reported being able to use his left arm in several ADLs that were previously impossible for him, such as buttoning his shirt and emptying the dishwasher with two hands. He felt more confident in using his upper extremity. [21]

This study demonstrates the potential of virtual reality technology to be an assessment and training device in stroke rehabilitation. It is important that the training routines are based on the patient's specific neurologic demands as detected during the virtual reality haptic assessment, the neurologic status evaluation, and the results of the occupational therapy assessment. A larger trial would be useful in determining the differences in improvement in motor ability of the upper extremities in stroke survivors using virtual reality in haptics. [21]

2.3 Motor Learning for Healthy Subjects

Many studies previously conducted have aimed to provoke motor learning in subjects with no known history of musculoskeletal or neurological disorders. The results and protocol to these studies are significant when applied to cases where the subjects participating demonstrate motor disabilities. The benefits can be extended to aiding in the recovery of multi-joint arm coordination, which was lost due to brain injury, or in gaining motor skills in the workplace or athletics. They can also be useful in designing future research and discussing progressions made in this research field. This research is applicable to these studies because the participating subjects lack motor deficiencies.

In one study, which 12 subjects with no known neuromotor disorders participated in, the ability of unimpaired humans to adapt to a perpendicular, viscous, force-field environment was examined. They were to perform a series of 20 cm, half-second reaching movements using their dominant arm while holding the handle of a two-joint robotic manipulator. The movement was conducted in the horizontal plane and they were to reach from a beginning target to an end target in a half-second. A sling hung from the

ceiling supported the subject's arm against gravity and a Velcro torso support restrained their shoulders. A cursor on an overhead monitor displayed their hand position and a computer supplied qualitative feedback of the movement duration after each trial. The force-field gains were unpredictable and uncorrelated from one trial to another. A perpendicular viscous field was created to deflect the hand perpendicularly from its intended path with a force that was proportional to the hand velocity along its path. [22]

Two random perturbation series were incorporated into two different experiments. In experiment 1, four subjects were to complete 200 trials where the force-field gain followed a Gaussian distribution. The sequence in this experiment was designed to ensure that there was insignificant correlation between perturbation magnitudes on consecutive trials separated by over 40 trials. The subjects experienced the same sequence of perturbations. In experiment 2, eight subjects were exposed to a series of 400 trials with a bimodal probability density function. The bimodal function was created by shuffling together two unimodal sequences, each with individual Gaussian distributions with means of 6Ns/m and 25 Ns/m. Each of subjects completed the same series of trials. [22]

Kinematic and kinetic behavior measures were taken to evaluate each subject's motor performance for each trial. One measure calculated was "movement error," which was the peak deviation of the hand from a straight-line trajectory passing between the initial and final targets. This measure was utilized to analyze kinematic performance. [22]

The results of this study showed that subjects adapted their motor behavior in response to the random sequence of force field gains. They compensated for the

approximate mean field of the stochastic sequence, not the most likely field. They also compensated using memories of only the most recent perturbations and performances. During the experiments, subjects experienced forces that were directed toward the left. In both experiments, subjects made hand-path deviations that were toward the right to oppose the anticipated forces. Also, movements that were performed in the stronger than average force-fields were undercompensated and movements performed in the weaker than average force-fields were overcompensated. This suggests that subjects were compensating for the average perturbing force-field in both experiments. The learning rates achieved during this study were significantly faster than those achieved in consistent viscous environments when subjects were required to reach in several different directions. The results to this study also show that an adaptive process compensated for the approximate mean field gain from each sequence of perpendicular viscous force. The subjects did not adapt to the most frequently induced force and adaptation did not depend on the particular distribution of perturbations. When motor performance that depended only on movement error and perturbation gain from the previous trial was modeled, it was seen that a significant amount of movement error was reduced and allowed for a quick and appropriate response to long-term changes in the distribution of perturbations. Therefore, this study supports the belief that neural structures modified as a result of motor adaptation do not clearly retain memories of performances or perturbations beyond one or two previous trials. [22]

Another study investigates if the use of a robot is capable of modifying healthy subjects' hand movements to a pre-selected trajectory. People are able to recover their original kinematic patterns when they are continuously exposed to a robot-generated

force that steadily disturbs arm motion. This is possible because they cancel out the robot-generated forces with a preplanned pattern of forces, which is known as feedfoward control. Feedfoward control is demonstrated when the interruptions are suddenly removed and the subjects make movements in the direction opposite to the interfering forces. [23]

This research included eight healthy right-handed adults with no history of orthopedic or neurologic disorders. They were seated so the range of targets was anterior to the shoulder while holding a two-degree-of-freedom manipulandum. A computer monitor was located in front of their eyes and displayed consecutive visual targets to initiate distinct movements. Each movement was 10 centimeters in one of three directions, anterior-right, anterior-left, or posterior-chest. Data were collected at 100 Hz. [23]

The subjects each completed 873 movements, which were divided into separate phases. The first phase included 15 movements to become familiar with the system (unperturbed familiarization phase). Then a baseline pattern was established with 15 movements in the unperturbed baseline phase. Next, a machine-learning phase was completed in which 298 movements with random perturbations were present one in four trials. The fourth phase included 18 movements to verify whether the baseline pattern was altered (unperturbed baseline phase). The learning phase was next, in which 330 movements with a constant exposure to forces was completed. Next, 120 movements with random removal of the force for one in eight trials was completed to determine any after-effects. Finally, a washout phase was completed where 75 movements without any forces were done. The subjects were to move in a curved, sinusoidal-shaped trajectory.

This trajectory was chosen because it is not a biomechanically or physiologically impossible motion and the forces it involves can be learned in a reasonable amount of time. [23]

To determine the degree of shift of the subjects' movements towards the desired trajectory, the error between the desired and actual initial vectors was measured. This was called the initial direction error. One of the main analyses of this study was to determine whether or not the subjects' movements could be shifted towards the desired trajectory as an after-effect of adaptation. The after-effects occurred when the robotic forces were removed. The results show that subjects' after-effect trajectories were constantly significantly moved towards the desired trajectory. This shift was not complete; there was a notable amount of residual differences between the desired trajectories and the after-effects. The method used to achieve such results did not assure a lasting result of these effects, which is not unexpected because the subjects were not told in any way to sustain the after-effect. Also, the speed profiles of the after-effect trajectories never were similar to the single, bell-shaped curve of the desired trajectory. [23]

A second experiment was completed with four additional subjects. They repeated the same experiment, except there was only visual feedback of hand position during motion in the initial, undisturbed movements. After the movement was completed, visual feedback was given to show the location of the cursor and to move it to the appropriate starting point for the next movement. [23]

The results to this portion of the study demonstrate that the washout of the after-effect of the adaptation was diminished, although it was not totally removed. The

subjects learned very similar trajectories in both experiments; however the after-effects decreased more slowly without visual feedback. The first experiment, which allowed visual feedback, was less variable and therefore suggests that visual feedback aids in control and the learning of a movement. [23]

A third portion of this study, which included four additional subjects who completed a slightly different procedure, was conducted. They were to complete extra trials in more directions during the baseline, after-effects, and final washout segments. These trials were aimed at targets that were located halfway between the original targets. [23]

The results to this portion of the study show notable after-effects in the nonpracticed directions, which suggest that their learning was generalized to movements that were not practiced. The after-effects from this portion of the study were less notable. Although there were considerable after-effects that generalize to nearby locations these effects diminish with their distance from the practiced trajectories. [23]

The goal of this study was to research an implicit approach to robot-aided motor learning. The subjects were to complete repeated reaching movements of the hand with the occurrence of disturbing forces. The perturbing forces were designed so that when they were removed, a desired trajectory was achieved as a result of the after-effect of adaptation. Although no instruction was given to do so, the subjects shifted their motion toward the desired trajectory. Therefore, the nervous system was "tricked" into generating a new motor command. This study does not argue that it is beneficial for motor learning to withhold information of a preferred performance from the subject; it only suggests that no clear goal is required to obtain a particular effect. [23]

Another article studied the effects of trial-to-trial, random variation in environmental forces on the motor adaptation of healthy human subjects during reaching. Twenty-four subjects with no history of neurological or musculoskeletal impairment participated in this study. They were seated with their hand attached through a splint to a robot arm while they were to reach alternately to two target light-emitting diodes. The targets were positioned in front of both shoulders just inside the boundary of the reaching workspace. After each movement, the computer provided qualitative feedback regarding the reach speed of the movement (too fast, too slow, just right = 1.2 seconds). The robot produced a velocity-dependant force field, which was applied only during the outward reach. For right-handed subjects, the force was directed leftward and perpendicular to the hand velocity. For left-handed subjects, the field and movement analyses were mirror symmetric. [24]

In order to differentiate adaptation to a randomly varying environment, the study was designed so that the same subject was initially exposed to a predictable environment and then to a random environment. Within each of three groups, the subjects' performance was compared. In the first group, the subjects participated in five stages of movements. In the first stage, null field 1, the subject performed 40 reaches without any applied robotic forces. In the next stage, the mean field, the subject completed 60 movements while the robot exerted a constant force that produced a leftward disturbance of the hand. The third stage, null field 2, involved 20 reaches with no forces involved. This stage was included to measure the after-effect of adaptation in the mean field. In the fourth field, noise field, 60 reaches were completed with varied forces. A slightly different magnitude of force was exerted for each reach, but the average magnitude was

the same as that of the mean field. The final stage, null field 3, consisted of 20 reaches without any forces involved. [24]

The second group of subjects completed a similar sequence of repetitions. However, rather than being exposed to the noise field in the fourth stage, they completed another block of mean field disturbances. The third group of subjects completed the noise field first, and then the mean field. This was done to check for possible effects that may occur due to ordering. [24]

The results of the first group show that when the robot began exerting forces in the mean or noise fields there were large errors which were followed by a slow, steady recovery of their original performance. When the forces were removed, the subjects showed after-effects, such as increased reaching error in the direction opposite to the force field. The magnitude of the after effects slowly decreased with repeated movements. Although there were decreased after-effects following the noise field, the group's performance in the mean and noise fields were not notably different regarding average final error and the variance of error. Also, they demonstrated similar rates of performance improvement in the random and mean fields. This occurred despite the fact that one stage had random perturbations and one had predictable perturbations and there was a diminished after-effect. This is most likely due to an increase in arm impedance during reaching in the noise field, which is thought to occur because of stiffening of the arm about the reference trajectory. These subjects utilized the most recently stored dynamic model to estimate the average of the random field. However, the ability to form a model of the random field did not depend on previous exposure to the mean field. The results for the third group of subjects showed that they formed an internal model of the

random field, which is demonstrated by a minimization of error over the last 40 reaches. [24]

Three major ideas can be concluded from this study. First, significant variability in an environment containing perturbations does not prevent the development of internal models of limb dynamics. The subjects were able to compensate for the mean of the random disturbances in the environment. Therefore, the model is most likely formed over a moving average computation and may operate over only a few previous reaches. Next, the results to this research suggest that impedance control can coexist with the application of internal models for control. So, when learning to move in a random mechanical environment, impedance is augmented while internal models are created. Lastly, it was found that when realistic models of motor adaptation are created, their structure should incorporate two adaptive processes; internal model formation and impedance regulation. This is an important goal for future research. [24]

The goal of another study was to research the stability of behavioral changes related to the adaptation to an external force field. The experimental method allowed the removal of the external force while simultaneously minimizing the occurrence of kinematic after-effects. Eleven subjects with no known history of neuromotor disorders participated in this study. They were to make goal-directed movements in the horizontal plane while holding the handle of a two-joint, robotic manipulator. The position, velocity, and acceleration of the handle were calculated from position encoders that were used to record the angular position of the two robotic joints. Two torque motors within the robot created both a viscous field and the mechanical channel field. The subjects'

arms were supported against gravity and their shoulders were restrained with a Velcro torso support. [25]

Visual "beginning" and "end" targets were displayed on a computer monitor located above the manipulandum. The targets were separated by a distance corresponding to 20 cm in the plane of the arm and were located along the line passing through the center of rotation of the subject's shoulder. The location of the hand was displayed on the monitor as a cursor and was visible to the subject. The subjects were to reach from the "beginning" target to the "end" target in a half second and then they were to rest while the manipulandum moved the hand back to the "beginning" target. The computer provided qualitative feedback regarding the movement speed (too fast, too slow, just right; 0.45 to 0.55 s). After every 200 movements, the subject was allowed to rest briefly (~ two to three min). This procedure was created to allow the subject's to experience the limb's mechanical environment along a limited set of trajectories. [25]

Three mechanical environments were presented to the subjects, a null field, a perpendicular field, and a channel field. During the null field, the torque motors produced an output of zero torque. During the perpendicular field, a perpendicular force that was proportional to the velocity of the hand was delivered to the hand. This environment took place during the adaptation phase of the experiment. In the channel phase of the experiment, the subjects moved in a stiff mechanical guide along the straight-line path between the beginning and end targets. This phase constrained the hand path of the subject; however they were free to move at any movement speed and with nearly any force. The channel phase succeeded in reducing the kinematic consequence of any perpendicular force exerted by the subject. [25]

The subjects were separated into two groups, a test group and a control group. The experiment was conducted in six phases. In the first phase, each subject completed 100 null field movements. Next, 100 channel movements were completed. The third phase included another 100 null set movements to reemphasize the initial conditions after the channel movements. The purpose of the first three stages was to reveal the subject's unadapted motor behavior in both the null and channel environments. The fourth stage included 150 movements in the perpendicular field, which disrupted subjects from their unadapted pattern of limb control. The fifth phase differed for the two groups. Six out of seven subjects in the test group were to make 150 channel movements and subjects in the control group were to complete 150 alternating channel and null field movements. The seventh subject in the test group completed a truncated version of the test group procedure, which was done to study the effects of limited exposure to the mechanical channel environment. In the sixth phase, all subjects made 50 null field movements, bringing the movements to a total of 650. [25]

To analyze subject performance, simple measures of kinematic and dynamic behavior were used. Kinematic error was determined by averaging the unsigned, hand path error over the entire reaching motion. Hand path error was the deviation of the hand from a straight-line trajectory between the initial and final targets. To measure the dynamic performance, the peak hand force perpendicular to the direction of the movement was calculated. This method of measurement provided evidence of motor adaptation without exposing subjects to periodic "catch trials," which is a null field interjected in a block of trials where the endpoint is significant. [25]

The results to this study show that when the kinematic errors were eliminated, the process of disadaptation was much slower than when the after-effects were allowed to take place. This means that even though kinematic and dynamic measures affect disadaptation, kinematic optimization occurs more quickly. The results to the six phases of the protocol show that following adaptation to the perpendicular field, subjects that were allowed to make movements with kinematic errors quickly regained their preadaptation performance. However, subjects who had been prevented by the channel from moving in a straight-line trajectory showed a persistence of adaptation that lasted approximately 100 or more movements. This suggests that subjects persist in adaptation to a perturbing environment when kinematic errors are artificially minimized, despite the fact that subjects are able to make the same movement with significantly less force at the hand. The control subjects experienced a greater loss of adaptation than the test subjects. It is believed that the learning of kinematic and dynamic transformations arise from two independent processes, therefore it is expected for the processes to have different properties. The gradual loss of adaptation exhibited by the test subjects may be caused by the action of a neuromotor mechanism optimizing an aspect of dynamic performance at a fairly slow rate. The rapid loss of adaptation shown by control subjects was controlled by an action of a separate mechanism optimizing kinematic performance. Through kinematic errors after adaptation, the channel constraint allows us to observe the action of a slower mode of neuromotor control that is typically hidden by the quick minimization of hand-path errors. The results of this study supply strong experimental evidence that both kinematic and dynamic measures influence motor adaptation of arm

movements to an external force. Kinematic-dependent factors seem to have a more significant role in the rapid loss of adaptation after restoring the initial dynamics. [25]

The studies discussed in this section discuss inducing motor learning in subjects with no known history of musculoskeletal or neurological disorders. This is significant because these procedures and therapies may be applied to existing therapies for subjects with motor deficiencies, particularly those who have suffered from strokes. With over 740,000 strokes occurring a year in the United States, they are the primary cause of motor disabilities and the principal cause of death. Motor recovery following a stroke is frequently incomplete; therefore motor deficits remain a primary cause of long-term disability preceding a stroke. Only 10% of stroke survivors recover nearly completely and 25% recover with minor impairments. Therefore, further investigating motor rehabilitation therapies for patients with musculoskeletal or neurological disorders is an important issue. As discussed in the following chapter, this research is aimed at designing therapy methods that incorporate haptics and virtual reality to provoke motor learning in subjects with no known motor disorders.

CHAPTER 3

METHODOLOGY

3.1 Purpose of Research

The purpose of this research was to utilize haptics and develop virtual environments to induce and evaluate motor learning in healthy subjects. Within several virtual environments different types of feedback were delivered and the most efficient in promoting motor learning is determined. The benefits of this study may be extended to enhance current motor rehabilitation treatments for patients with musculoskeletal or neurological disorders.

The Haptic Master permits three degrees-of-freedom while incorporating virtual reality, therefore allowing innovative studies to be performed on healthy subjects. The Haptic Master also has a higher haptic resolution (710 x 10^12) than other force controlled devices with the same force depth (1 x 10^4). Haptic resolution is the ratio of the workspace volume and the smallest object that can be felt. The force depth is the ratio of a normal force and the smallest change in force that can be felt. The Haptic Master's degrees-of-freedom, volume of workspace, and other factors are shown in figure 3.1.

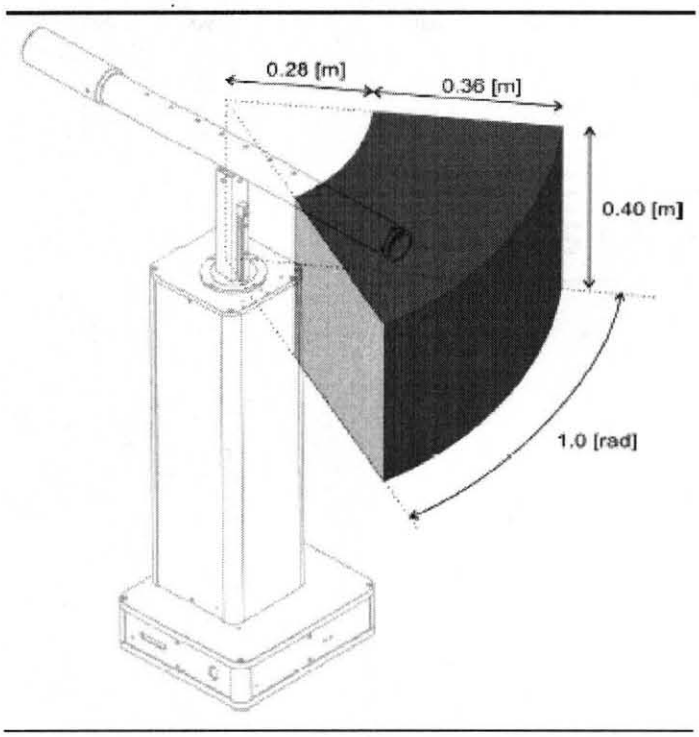

Figure 3.1 The Haptic Master has three degrees-of-freedom, which span a volumetric workspace. The volume of the workspace was created to fit most of the seated human tasks into this workspace.

Source: R. Q. van der Linde and P. Lammertse. [5]

3.2 Subjects

Three subjects (subject 1 was female and subjects 2 and 3 were males) with no history of musculoskeletal or neurological disorders participated in this research. All were right-hand dominant and under the age of 45 years.

3.3 Procedure

Three virtual environment scenarios were completed by the subjects. These environments were programmed by Qinyin Qiu. The subjects were to maneuver a sphere through an environment following an optimal trajectory to the best of their ability. The

virtual environment was created to be two dimensional. This was achieved by including a "floor" or surface for the subjects to maneuver along, which restricted their movements to the YZ plane where Y was oriented horizontally and Z was oriented vertically.

The first condition was a cube maze, as shown in figure 3.2, where visual feedback was given. The visual feedback allowed the subjects to see the sphere they were moving through the maze at all times during the experiment. In the second scenario, the same cube maze was completed with no visual feedback. The lack of visual feedback did not allow them to see the sphere's location during therapy. The sphere was only visible between trials when the subject was to move from the end point to the start location. Within the cube maze, the subject was to maneuver from the red circle, which was marked as the start point, to the opaque back wall. They were to follow the optimum trajectory (displayed in red) to the best of their ability. Force feedback was delivered only from the walls of the three blue cubes in the environment. The aqua surface is the bottom of the maze and provided a flat surface to move along but did not give force feedback.

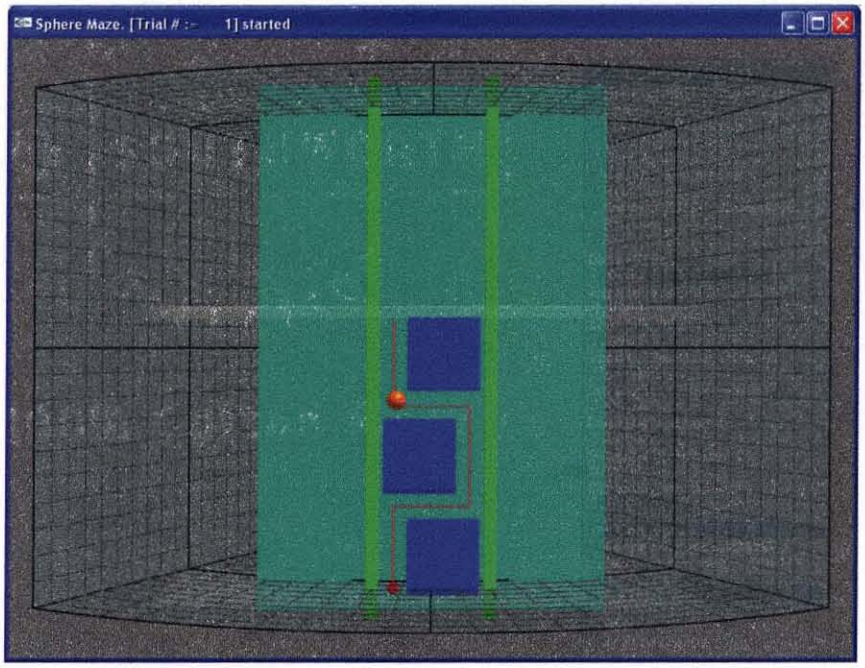

Figure 3.2 A picture of the maze, from a front view. The maze is composed of three cubes and two side walls.

Source: Qinyin Qiu. [26]

In the last scenario, the subjects maneuvered through an environment where the goal was to follow a linear trajectory, as shown in figure 3.3. There was no visual feedback provided in this case. Therefore, as in the second scenario, they were not able to see the location of the sphere at any point during movement within the virtual environment, except for between trials. They were to maneuver between the two vertical green walls, which were rotated around the x-axis by -3.600 degrees, following a linear trajectory to the best of their ability. The start location was in between the two green walls at the bottom of the maze and the end was reached when they hit the opaque wall at the top of the environment. Force feedback was delivered from the green side walls. In this environment, the aqua surface also represented a flat surface to move along where no forces where delivered from. There was no optimal trajectory displayed in this scenario.

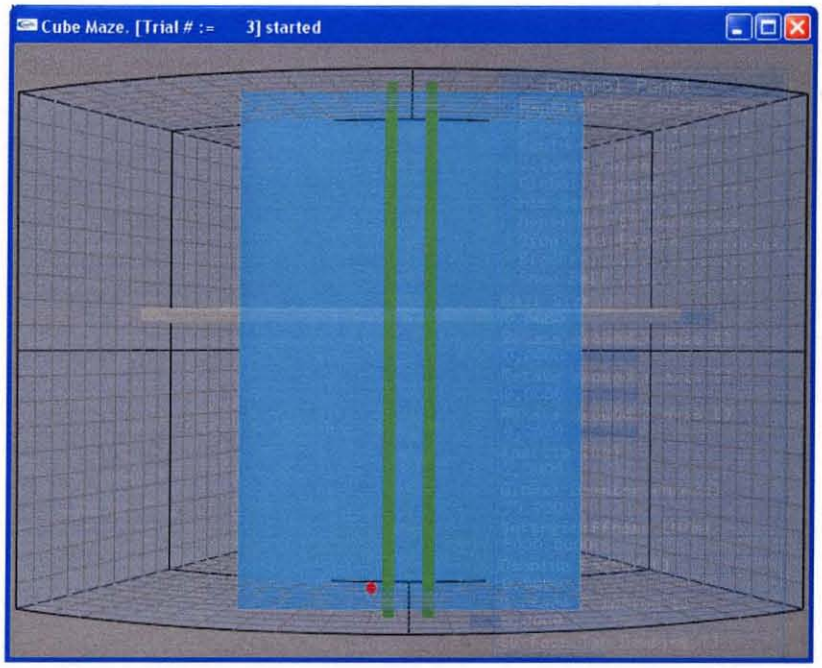

Figure 3.3 An image of the linear trajectory. The maze is only composed of two side walls.

Source: Qinyin Qiu. [26]

Within each of these three conditions, two types of haptic feedback were delivered by the Haptic Master. They were known as "no blocking' and "blocking". These three scenarios were completed twice on separate days by the respective number of subjects, one day with no blocking feedback delivered and one day with blocking feedback delivered. During no blocking force feedback, movement was restricted to a narrow area surrounding the optimal trajectory in the channel between the cubes or linear walls. They were able to move along the cube walls or side walls of the linear trajectory; however the friction delivered by the Haptic Master made this movement more difficult than when in the channel between walls. As subjects increased the force with which they moved the sphere along the walls, a higher force feedback was returned.

During blocking feedback, in order to move throughout the environment, the force vector had to be directed towards the optimal trajectory. Therefore, when the subject moved the sphere into the cube walls, they were not able to continue movement along the walls. They had to redirect their movement so that the force trajectory was oriented towards the optimal trajectory, which forced them to move the sphere back towards the pathway between walls. This allowed time for the subjects to reconsider and reprogram their movement.

The following graphs display two examples of the forces produced by the two feedback scenarios. The Z oriented force is shown, which is directed vertically. In the no blocking graph (figure 3.3), three wall hits are illustrated by the three sharp peaks. These peaks represent the brief increases in force that occur. The magnitudes of these forces are higher than those from the blocking feedback. There are two peaks in the blocking feedback, representing two hits into the walls. These peaks are noisier than those in the no blocking graph, due to the forces received from the Haptic Master. More accelerations and forces are seen in the graph prior to these two peaks than in no blocking feedback. In the blocking feedback scenario, the peaks are occur farther apart and later than with no blocking because the subject requires a longer period of time to maneuver through the maze.

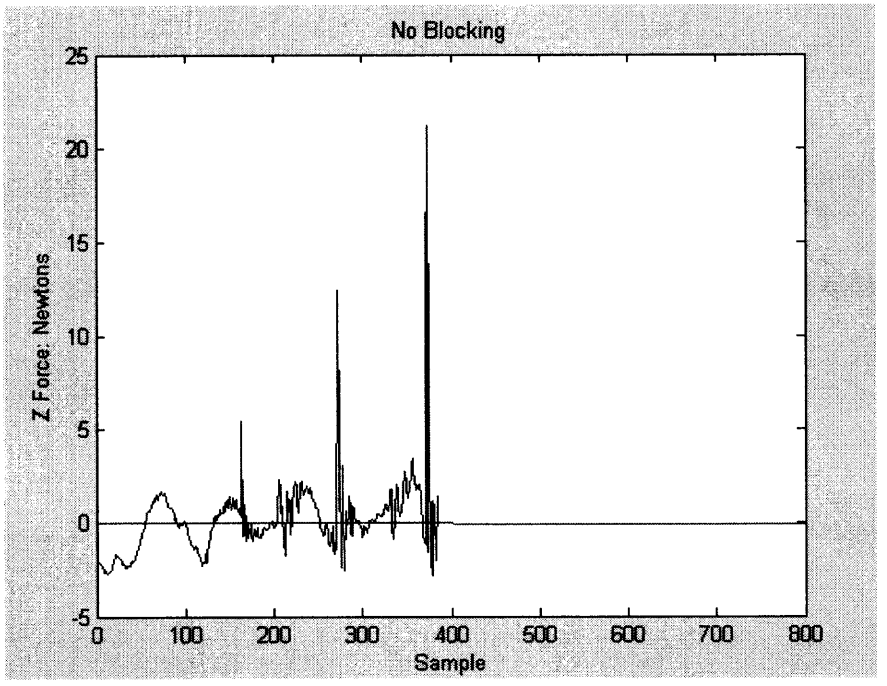

Figure 3.4 Vertical forces produced by the no blocking feedback versus time.

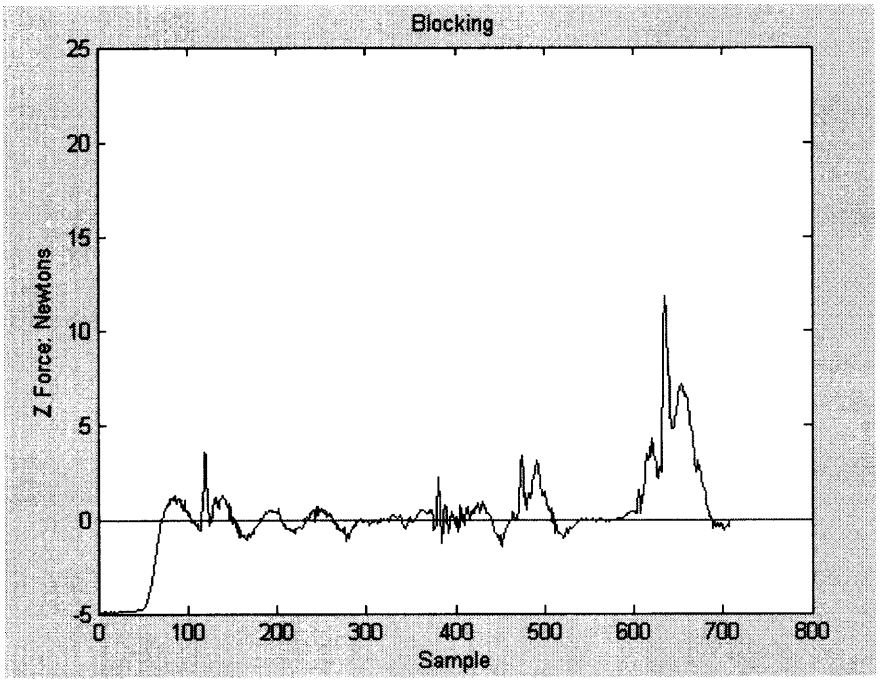

Figure 3.5 Vertical forces produced by the blocking feedback versus time.

Throughout these different conditions, certain procedures were always followed by the subjects. During testing, each subject remained seated in a stable chair positioned

behind the Haptic Master and in viewing distance of the computer monitor. While the controlled sphere was located at its start point within the virtual environment, the horizontal distance from the subject's shoulder on their right side of the body to the center of the Haptic Master's handle was recorded to ensure seating location consistency. The Haptic Master's location on the floor was also marked for constancy. The subjects were to maneuver through the maze using their dominant hand.

Prior to beginning the actual activity, the subjects were instructed to briefly familiarize themselves with the Haptic Master and the virtual environment. The orientation of the environment was altered to avoid any learning from occurring prior to the actual experiment. At the start of each trial within the experiment, the subject was verbally prepared by an experimenter who initialized each trial. A beeping sound prompted the subject to begin. At the end of each trial the Haptic Master automatically stopped recording data when the sphere reached the back wall.

Throughout all conditions, a set of five test trials through the virtual environment with no haptic feedback received was completed. Following this, 15 trials were completed as a training phase that delivered haptic feedback to the subject. This cycle of testing and training phases was repeated until 85 trials were finished. Rest between testing and training segments was minimal, lasting approximately 10 seconds. The completed trajectories following each trial were not displayed, eliminating some visual feedback from the experiment. At the end of each trial, they were to go from the endpoint to the start point by moving the sphere above the surface of the maze to prevent any additional training from occurring.

3.4 Data Collection and Analysis

The Haptic Master collected 10 data values, time, x, y, and z coordinates for position, x, y, and z coordinates for velocity, and x, y, and z coordinates for force. Matlab was used to analyze these data and compute learning parameters. Values within each subject's results and across all subject's results were compared.

The deviation of each trial's trajectory from a predetermined optimal trajectory was the main learning parameter measured. This deviation is computed by measuring the area between the optimal trajectory and the actual trial's trajectory. Any variation in this deviation area that occurs throughout the experiments is studied. The optimal trajectory is composed of 6 points, P1= (0.012, -0.0325, -0.205), P2= (0.012, -0.0325, -0.135), P3= (0.012, 0.0325, -0.135), P4= (0.012, 0.0325, -0.05), P5= (0.012, -0.0325, -0.05), and P6= (0.012, -0.0325, 0.025). The optimal trajectory is three dimensional, however the trajectory can analyzed on a two dimensional basis because the x coordinates are the same within this trajectory. Since the subjects are moving on a flat surface within the virtual environments, the x coordinates of position from their data are the same as those from the optimal trajectory. In figure 3.6, the optimal trajectory within the cube maze is graphed on the YZ plane in red. Figure 3.7 displays an example of the deviation area in blue between the optimal and actual trajectories.

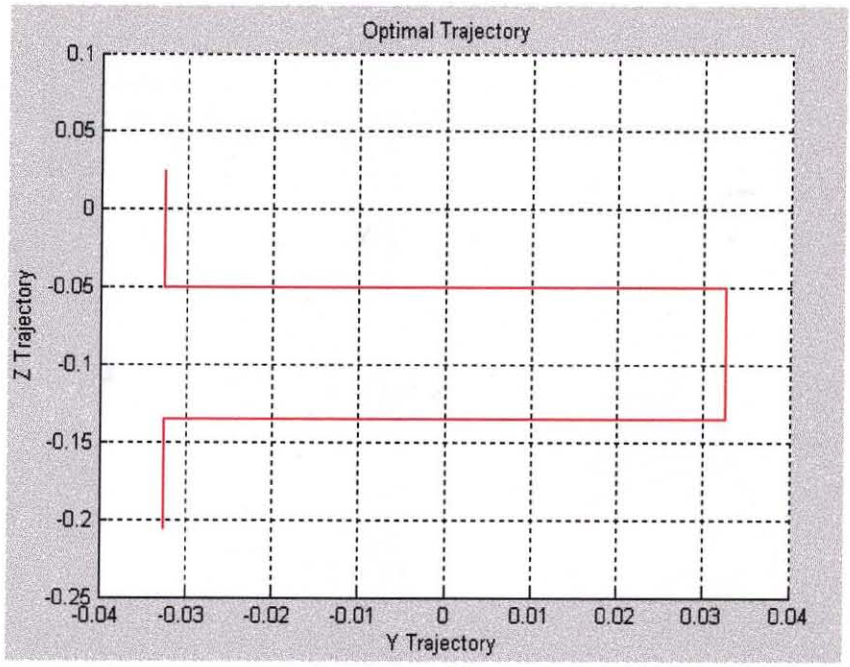

Figure 3.6 Optimal trajectory in the YZ plane.

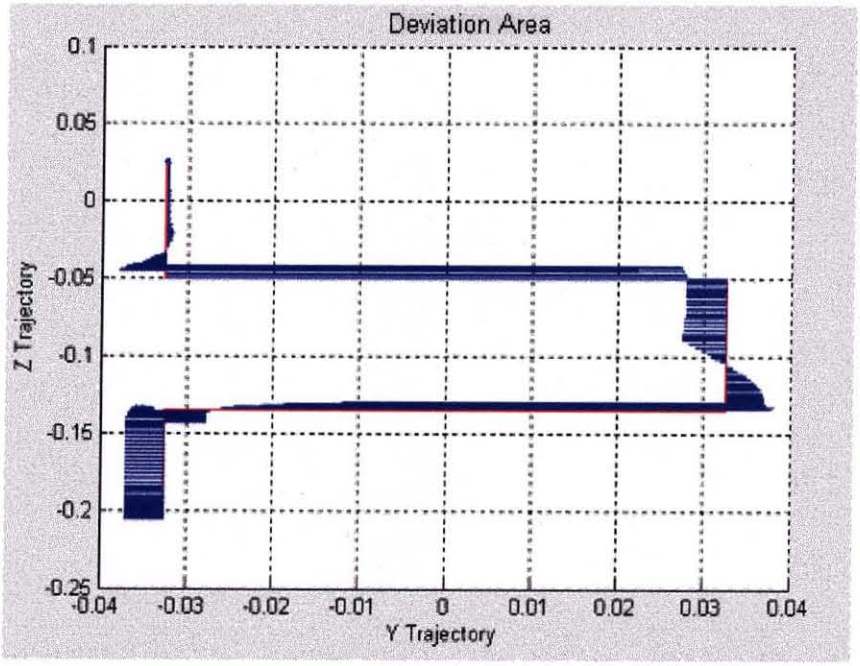

Figure 3.7 Deviation area between the optimal and actual trajectories.

A second parameter studied was the duration of each test trial's movement. This was considered to aid in determining whether any learning that occurred was motor learning or cognitive learning through analyzing decreases or increases in the time it took the subject to complete each trial.

CHAPTER 4

RESULTS

4.1 Cube Maze

4.1.1 Cube Maze With and Without Visual Feedback: Blocking Versus No Blocking

A statistical evaluation was performed on the data collected during the testing trials with the use of repeated measures analysis of variance (ANOVA) using StatView software. Data from the cube maze environment with and without visual feedback is initially analyzed together (as shown later in the chapter, the presence of visual feedback has no significant effect on learning). Results comparing the effect of blocking versus no blocking force feedback showed statistical significance, as displayed in figure 4.1 ($F(1, 2) = 183.980$, $p = 0.0054$). No blocking is shown to achieve a higher degree of learning, and therefore a lower average deviation area.

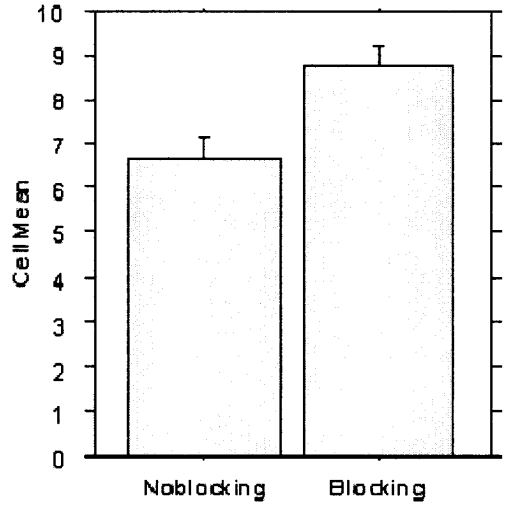

Figure 4.1 Bar plot for average deviation area versus the type of haptics delivered. (No blocking mean area = 6.647, blocking mean area = 8.691) (Error bars: ± standard error)

There is statistical significance of the test set number on the average deviation area ($F(4, 8) = 5.378$, $p = 0.0211$). The average deviation area decreases from the first to

the fourth test sets, as illustrated in figure 4.2. The subjects reported experiencing shoulder fatigue towards the end of the activity, therefore learning does not continue through the fifth test set.

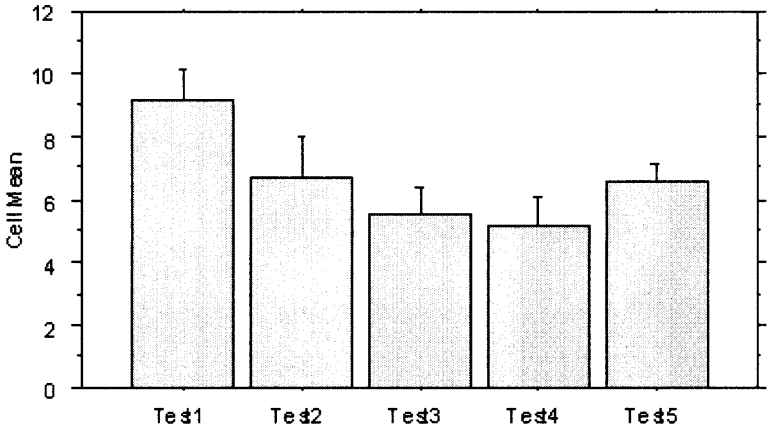

Figure 4.2 Bar plot for average deviation area versus each of the five test sets. No blocking haptic feedback is included in this evaluation. (Test 1 = 9.157, test 2 = 6.769, test 3 = 5.528, test 4 = 5.181, test 5 = 6.599) (Error bars: ± standard error)

There is no statistical significance of the test set on the average deviation area, when blocking feedback is present ($F(4, 8) = 0.481$, $p = 0.7489$). The average deviation area of the five test sets remains fairly constant throughout experimentation, as seen in figure 4.3.

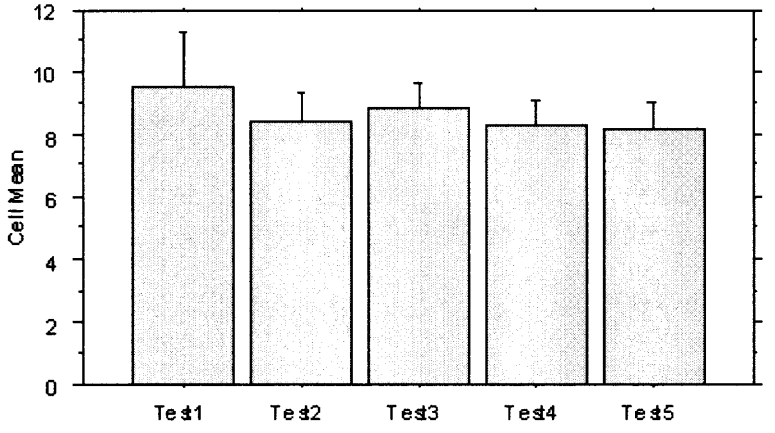

Figure 4.3 Bar plot for average deviation area versus each of the five test sets. Blocking haptic feedback is included in this evaluation. (Test 1 = 9.524, test 2 = 8.444, test 3 = 8.917, test 4 = 8.324, test 5 = 8.245) (Error bars: ± standard error)

The effect of visual feedback on learning in the no blocking condition is further illustrated in figure 4.4. The results to ANOVA show that visual feedback and the test set number do not have a significant effect on the average deviation area ($F(4, 8) = 0.203$, $p = 0.9298$). With and without visual feedback the deviation area decreases at a similar rate when no blocking force feedback is received. There is a visible decrease in the average deviation area as the test sets continue in both scenarios. Regardless of the presence of visual feedback, as the test sets progress from the first to fourth set there is a continuous decrease in the deviation area. This decrease does not continue to the fifth set, however, due to the subjects' verbally reported shoulder fatigue.

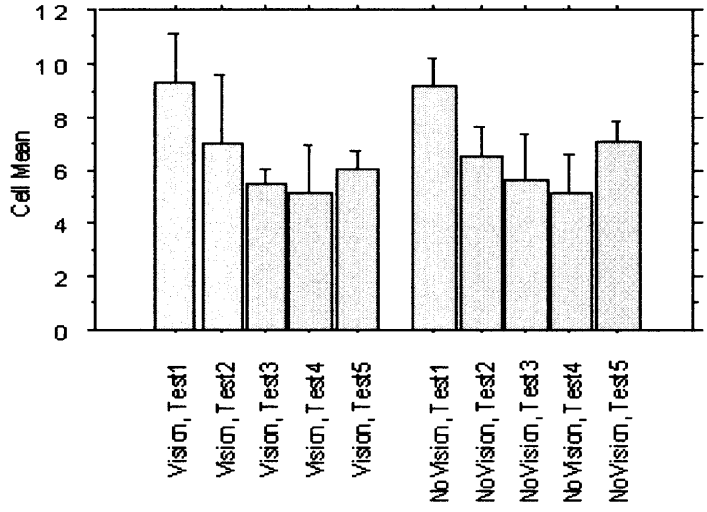

Figure 4.4 Bar plot for average deviation area versus each of the five test sets with no blocking force feedback and with respect to the presence of visual feedback delivered. (Error bars: ± standard error)

Figure 4.5 illustrates the inefficiency of blocking haptic feedback in improving the subjects' ability to follow the optimum trajectory, regardless of the presence of visual feedback. The results to the visual feedback x test set interaction effect are not statistically significant ($F(4, 8) = 1.964$, $p = 0.1933$). Although there is a slight decrease

in the average deviation area with the presence of visual feedback, this is not continuous throughout the test sets and the decrease is not as great as seen with no blocking haptic feedback. When there is no visual feedback, the average deviation area does not decrease at all throughout the activity.

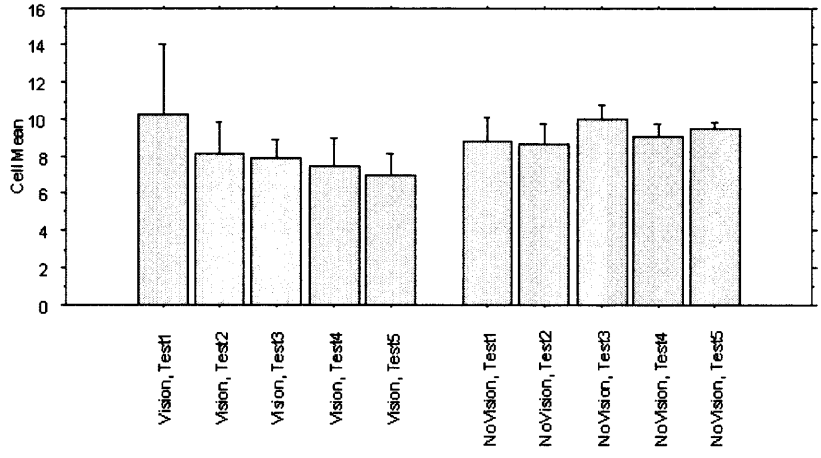

Figure 4.5 Bar plot for average deviation area versus each of the five test sets with blocking force feedback and with respect to the presence of visual feedback delivered. (Error bars: ± standard error)

Comparing results from the blocking and no blocking haptics both with and without the presence of visual feedback demonstrates that there is a larger decrease in the average deviation area when no blocking feedback is delivered to the subjects. Figure 4.6 shows a comparison between the force feedback scenarios across all subjects with visual feedback given. The average deviation area of each of the test sets among subjects is averaged and plotted for blocking and no blocking force feedback. Blocking force feedback produces an approximate decrease in the area between the optimal and trial trajectories of 28%; while no blocking force feedback produces a decrease of approximately 38% between the two trajectories. This percentage is determined by comparing the average deviation area from the first and fifth test sets.

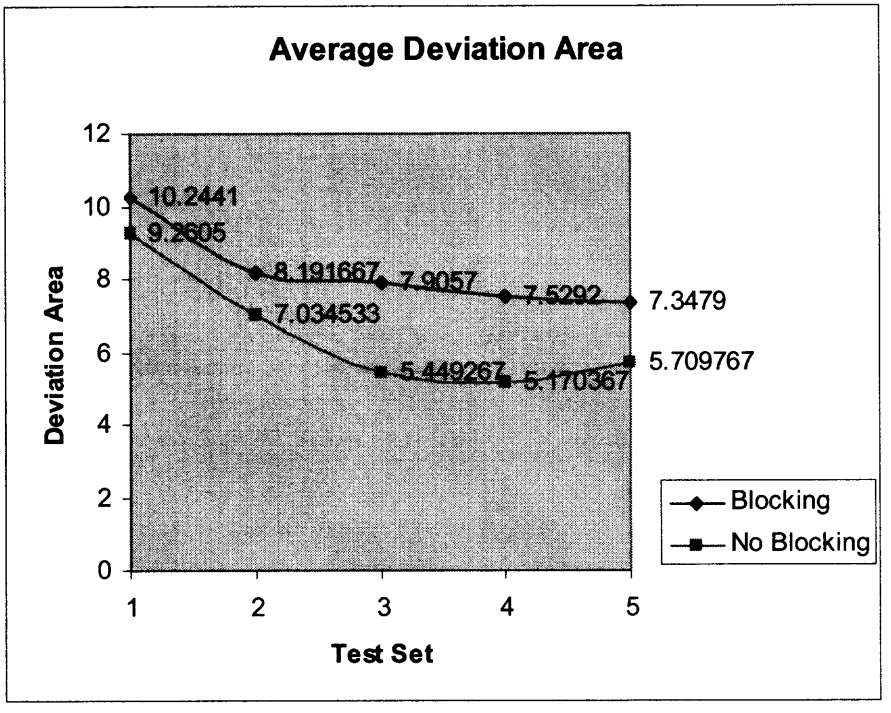

Figure 4.6 Average deviation areas with visual feedback from subjects 1, 2, and 3. The average of each of the five test sets from the blocking and no blocking force feedback is shown.

In figure 4.7, the results from blocking and no blocking haptic feedback are shown when visual feedback is not present. With blocking feedback, there is no learning and the average deviation area increases throughout the activity. However, no blocking force feedback produces a decrease in the area between the two trajectories of approximately 28%.

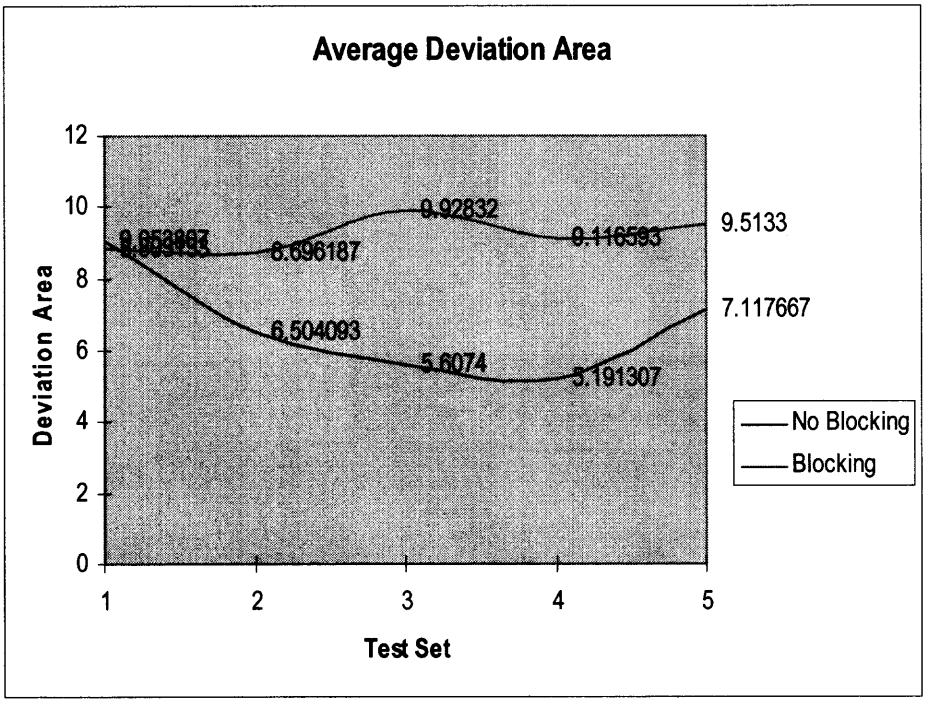

Figure 4.7 Average deviation areas without visual feedback from subjects 1, 2, and 3. The average of each of the five test sets from the blocking and no blocking force feedback is shown.

Overall, visual feedback does not produce a statistically significant effect ($F(1, 2) = 0.518$, $p = 0.5465$). In figure 4.8, it is shown that when visual feedback is given to the subjects, with either form of haptic feedback present, only a slightly lower deviation area is produced. The lack of effect of visual feedback is further illustrated in the previously described figure 4.4. In this bar graph, it is shown that the average deviation area decreases in the same manner regardless of the presence of visual feedback.

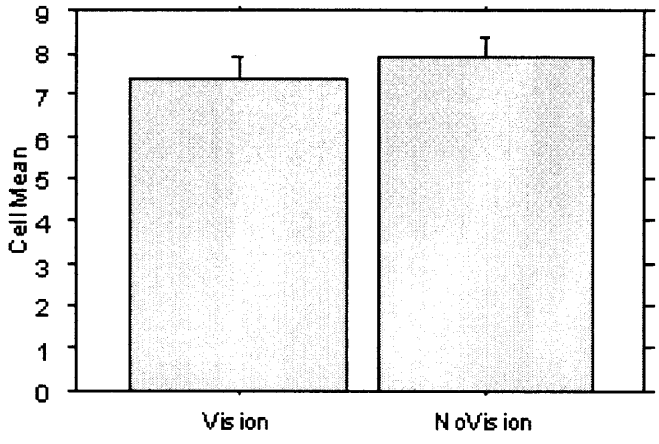

Figure 4.8 Bar plot for average deviation area versus the presence of visual feedback. (Visual feedback mean area = 7.385, no visual feedback mean area = 7.953) (Error bars: ± standard error)

4.1.2 Cube Maze: Movement Duration

The effect of several factors on the time required to complete test trials in the cube maze environment were compared using ANOVA. When the effect of the presence of visual feedback is analyzed it is determined to have no impact on the movement duration. As shown in figure 4.9, the average time required to maneuver through the maze is unaffected by visual feedback, regardless of the type of haptics received. The results to this comparison are therefore not statistically significant ($F(1, 2) = 3.533$ e-4, $p = 0.9867$).

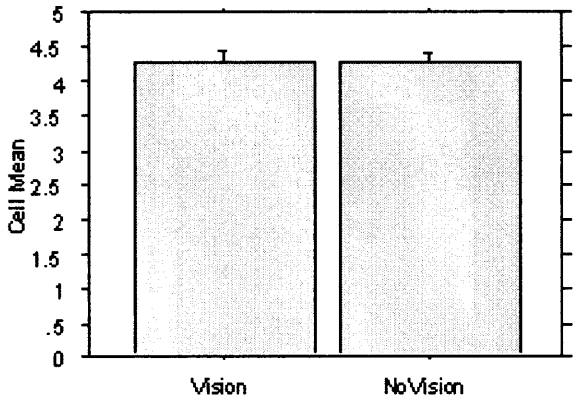

Figure 4.9 Bar plot for movement duration versus the presence of visual feedback. (Visual feedback mean area = 4.266, no visual feedback mean area = 4.268) (Error bars: ± standard error)

When the effect of the two types of haptic feedback present is compared to the movement duration, the results are as expected. The presence of no blocking haptic feedback allows the subjects to complete the maze at a faster rate than when blocking feedback is received. These results, which are shown in figure 4.10, are statistically significant ($F(1, 2) = 537.865$, $p = 0.0019$).

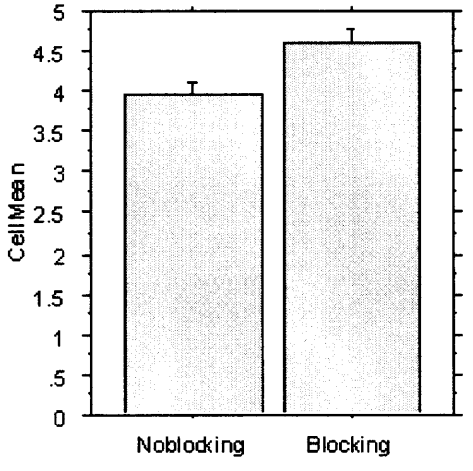

Figure 4.10 Bar plot for movement duration versus the type of haptic feedback delivered. (No blocking area = 3.949, blocking mean area = 4.585) (Error bars: ± standard error)

As shown in figure 4.11, the movement duration time does decrease as the test sets continue. However, this decrease is very minimal and not statistically significant ($F(4, 2) = 1.286$, $p = 0.3520$).

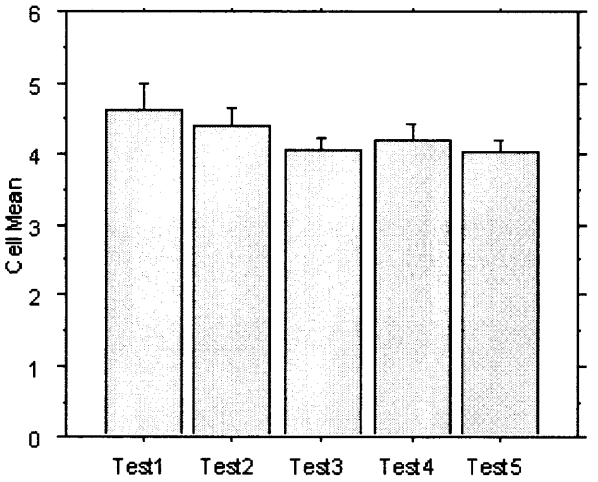

Figure 4.11 Bar plot for duration time versus each of the five test sets. Both forms of haptics are included in this evaluation. (Test 1 = 4.631, test 2 = 4.391, test 3 = 4.081, test 4 = 4.198, test 5 = 4.036) (Error bars: ± standard error)

4.2 Linear Trajectory with No Visual Feedback

4.2.1 Linear Trajectory: Three Subjects

Performing ANOVA on the data from all three subjects as a group shows there to be no statistical significance in the results. When the types of haptic feedback delivered are compared, it is seen again in figure 4.12 that no blocking force feedback produces a lower average deviation area that blocking feedback. However, this result is not statistically significant ($F(1, 2) = 4.909$, $p = 0.1571$).

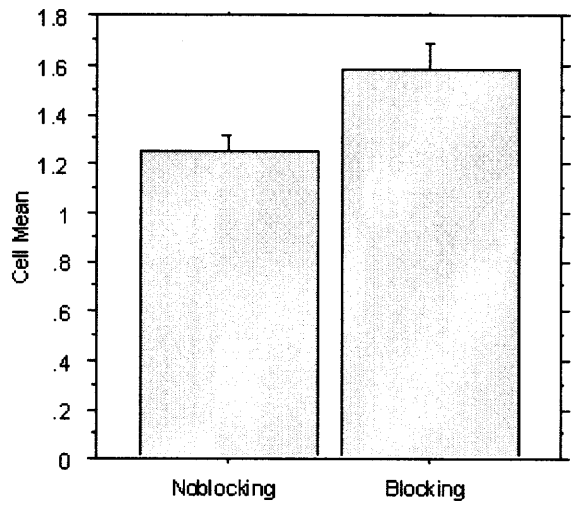

Figure 4.12 Bar plot for average deviation area versus the type of haptics delivered. (No blocking mean area = 1.251, blocking mean area = 1.584) (Error bars: ± standard error)

Figure 4.13 shows that there is a slight decrease in the average deviation area throughout the test sets, therefore there is some amount of learning occurring during the experiment. These results however are not statistically significant ($F(4, 8) = 2.819$, $p = 0.991$).

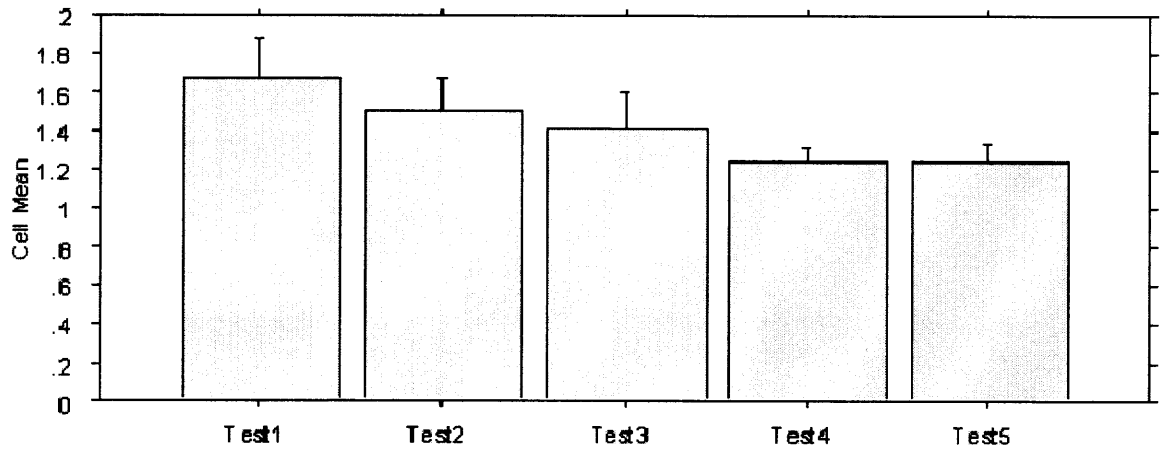

Figure 4.13 Bar plot for average deviation area versus each of the five test sets. Both forms of haptics are included in this evaluation. (Test 1 = 1.674, test 2 = 1.509, test 3 = 1.415, test 4 = 1.243, test 5 = 1.248) (Error bars: ± standard error)

Although small, there is a greater degree of learning that occurs with the presence of no blocking haptic feedback than with blocking feedback as illustrated in figure 4.14. These results are not statistically significant ($F(4, 2) = 0.410$, $p = 0.7974$).

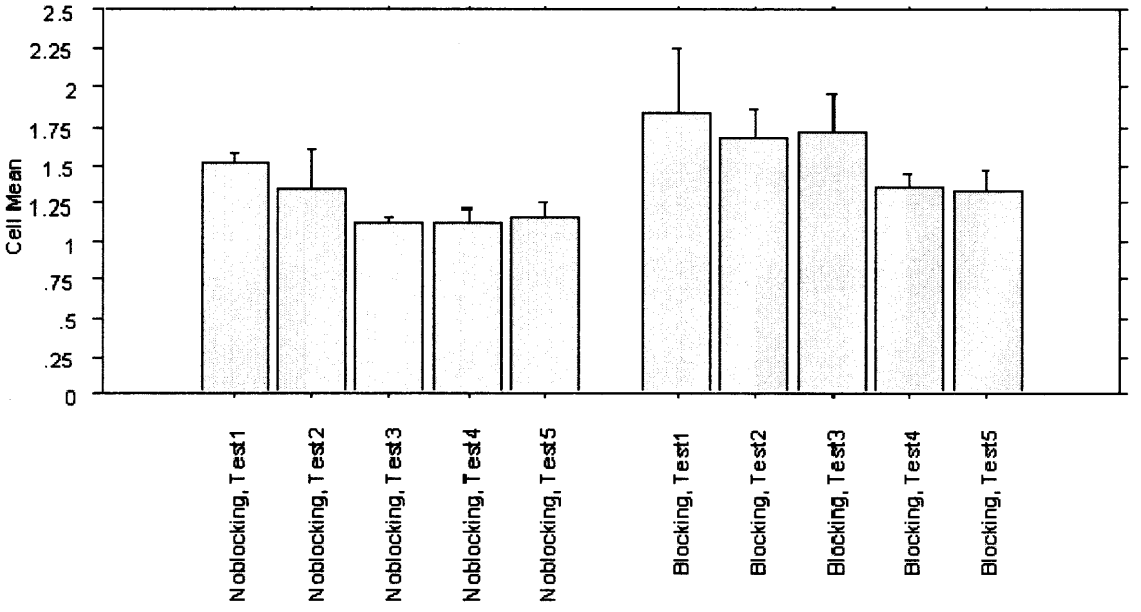

Figure 4.14 Bar plot for average deviation area versus each of the five test sets with respect to the type of haptic feedback delivered. (Error bars: ± standard error)

4.2.2 Linear Trajectory: Subject 1

Performing ANOVA on the data from each subject individually produces results that are inconsistent with those from analysis among the three subjects collectively. When comparing the effects of the two types of haptic feedback on the average deviation area, the results are statistically significant ($F(1, 4) = 14.668$, $p = 0.0186$). It is shown in figure 4.15 that when no blocking haptic feedback is received, subject 1 produces a smaller average deviation area between the optimal and test trajectories.

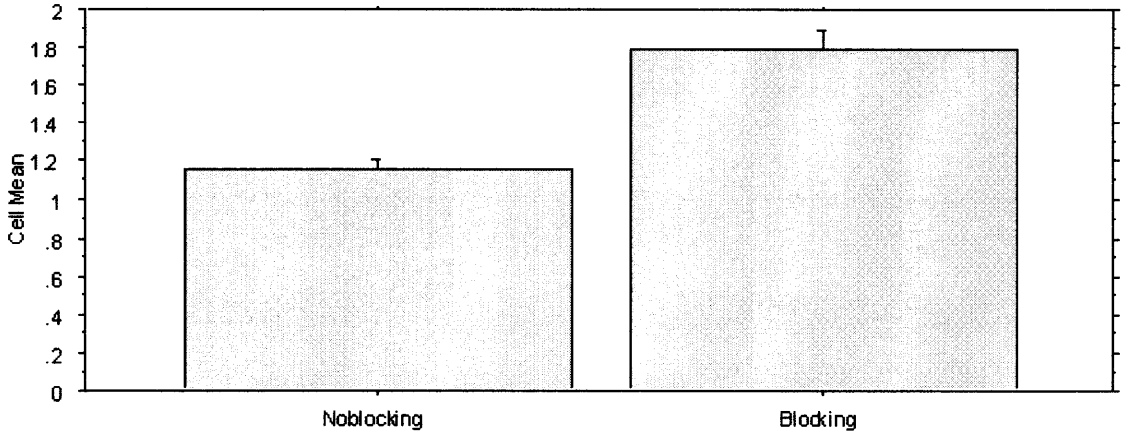

Figure 4.15 Bar plot for average deviation area versus the type of haptics delivered. (No blocking mean area = 1.162, blocking mean area = 1.791) (Error bars: ± standard error)

There is statistical significance between each learning set and the deviation area ($F(4, 16) = 9.040$, $p = 0.0005$). From the first to the fifth test set the average deviation area decreases. However, this does not occur at a consistent rate.

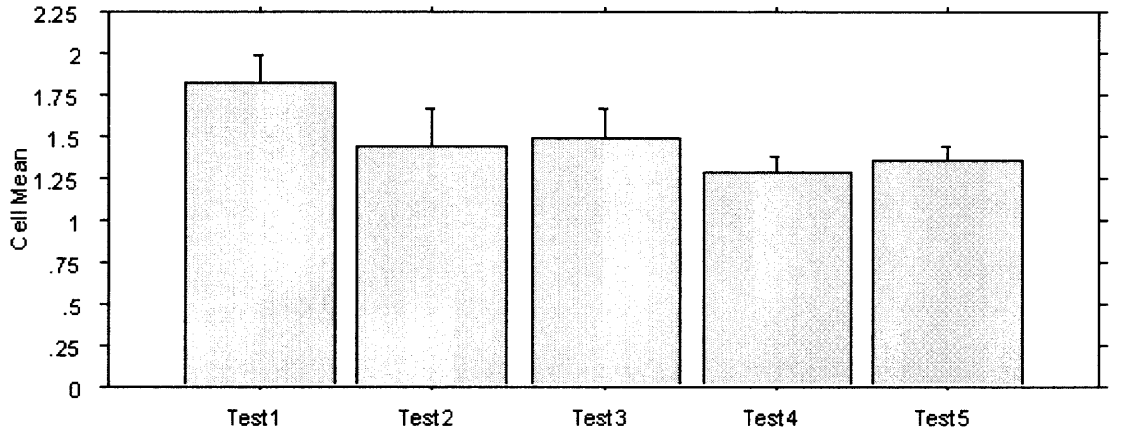

Figure 4.16 Bar plot for average deviation area versus each of the five test sets. Both forms of haptics are included in this evaluation. (Test 1 = 1.826, test 2 = 1.442, test 3 = 1.486, test 4 = 1.276, test 5 = 1.352) (Error bars: ± standard error)

There is a significant haptic feedback x test set interaction ($F(4, 16) = 4.620$, $p = 0.0114$). In figure 4.17, it is shown that blocking feedback produces a steadier decrease in the average deviation area than no blocking feedback. However, initially the blocking

feedback produces a higher deviation area than no blocking feedback. The fifth test sets have average deviation areas that are similar.

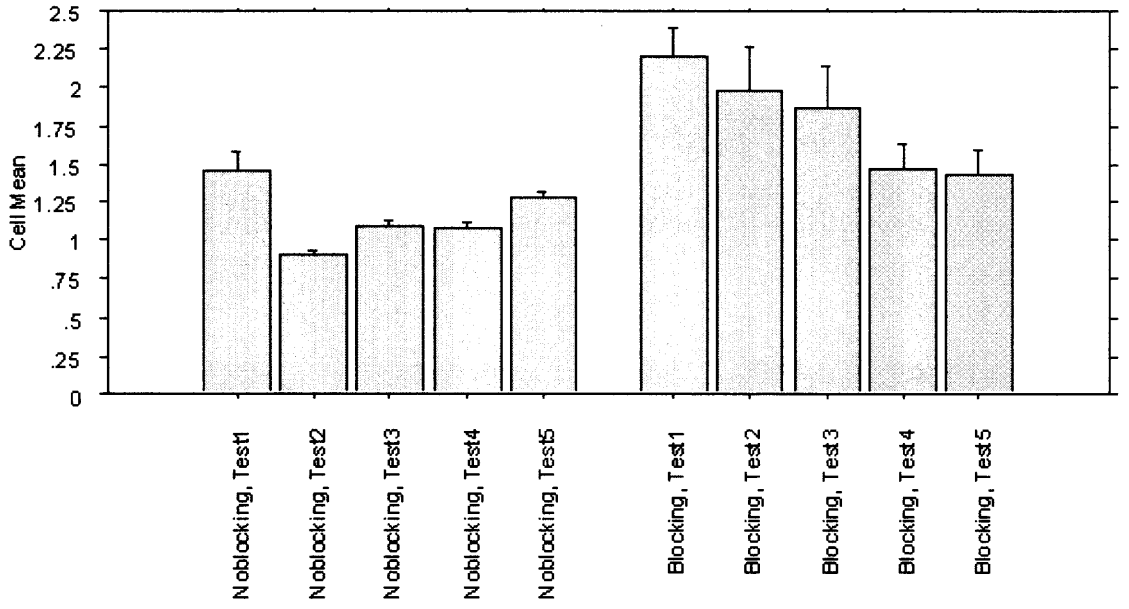

Figure 4.17 Bar plot for average deviation area versus each of the five test sets with respect to the type of haptic feedback delivered. (Error bars: ± standard error)

4.2.3 Linear Trajectory: Subject 2

When a statistical evaluation is performed to compare the type of haptic feedback and its effect on the average deviation area, there is no statistical significance ($F(1, 4) = 1.667$, $p = 0.2662$). Unlike previously illustrated results, as shown in figure 4.18, subject 2 produces a slightly lower average deviation area when blocking feedback is present. This may be due to the simplicity of this virtual environment. Unlike the cube maze, there are no turns within this environment which make movement difficult with blocking feedback.

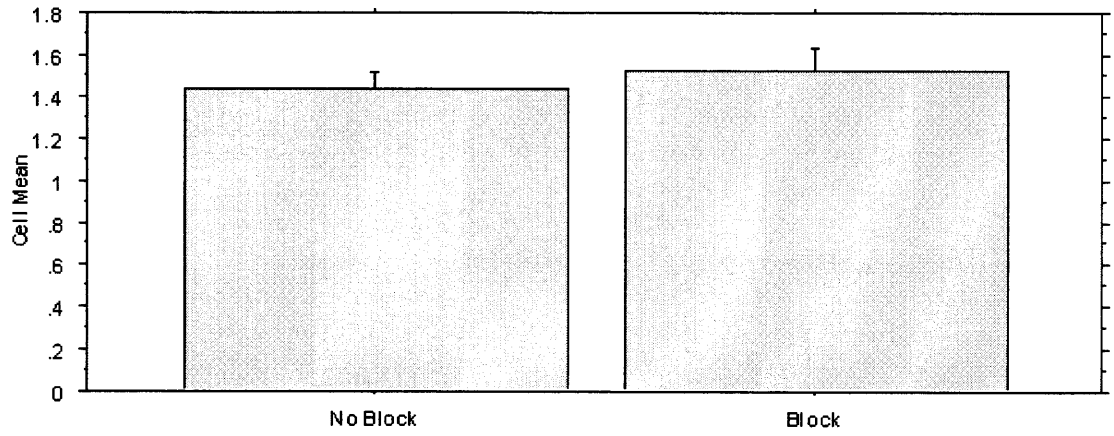

Figure 4.18 Bar plot of average deviation area versus the type of force feedback present. There is no visual feedback in this scenario. (No blocking mean area = 1.439, blocking mean area = 1.524) (Error bars: ± standard error)

There is statistical significance between each learning set and the deviation area ($F(4, 16) = 10.303$, $p = 0.0038$). As the test trials progress, the average deviation area decreases.

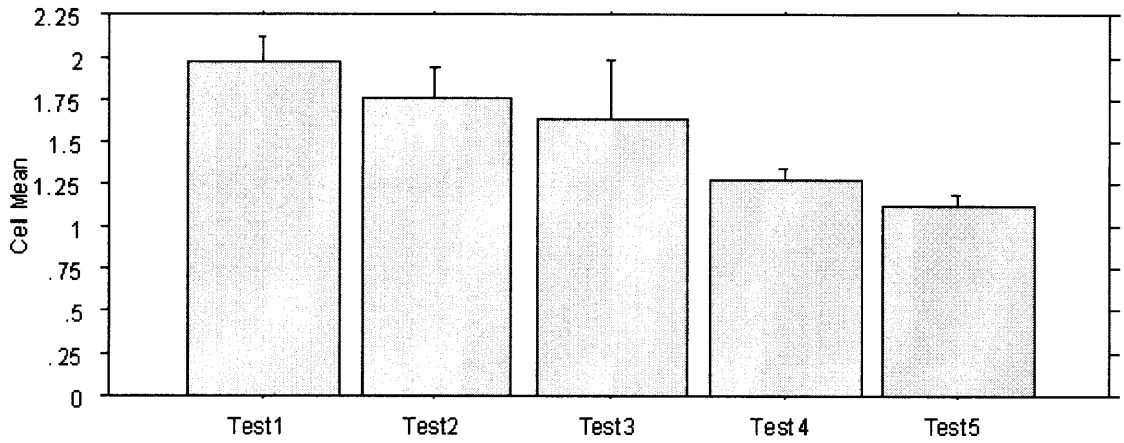

Figure 4.19 Bar plot for average deviation area versus each of the five test sets. Both forms of haptics are included in this evaluation. (Test 1 = 1.958, test 2 = 1.772, test 3 = 1.267, test 4 = 1.280, test 5 = 1.123) (Error bars: ± standard error)

There is a significant haptic feedback x test set interaction ($F(4, 16) = 5.561$, $p = 0.0053$). In figure 4.20, it is shown that blocking feedback produces a steadier decrease

in the average deviation area than no blocking feedback. However, the last test trials do have average deviation areas that are similar.

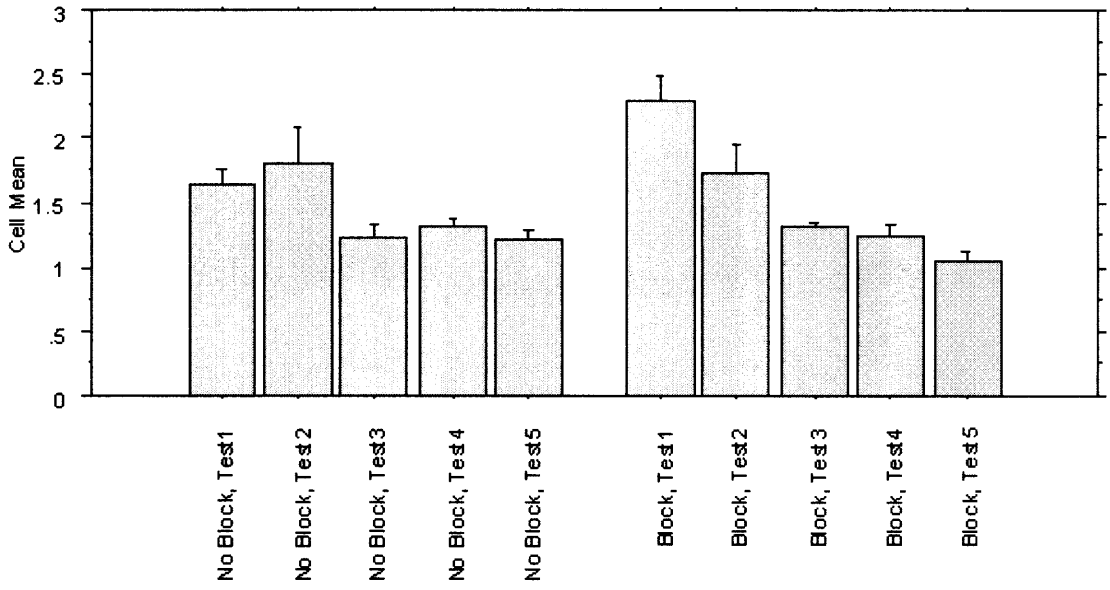

Figure 4.20 Bar plot for average deviation area versus each of the five test sets with respect to the type of haptic feedback delivered. (Error bars: ± standard error)

Figure 4.21 shows the difference in the results from blocking force feedback from subject 2's experiments. The bar graph on the left is from the cube maze with visual feedback and the one on the right is from the linear maze without visual feedback. It is clearly shown that within the linear environment, there a steadier, larger amount of learning.

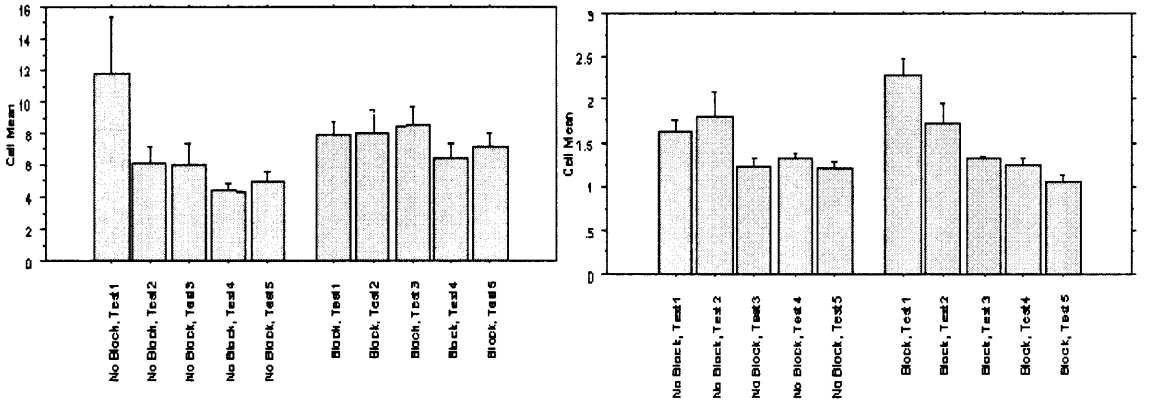

Figure 4.21 Bar plot for average deviation area versus each of the five test sets with respect to the type of haptic feedback delivered. Left: Subject 2 cube maze with visual feedback. Right: Subject 2 linear maze with no visual feedback. (Error bars: ± standard error)

4.2.4 Linear Trajectory: Subject 3

The results from subject 3 are different than those seen from the previous two subjects. It is shown in figure 4.22 that no blocking haptic feedback does produce a slightly lower average deviation area, these results are not statistically significant ($F(1, 4) = 3.785$, $p = 0.1236$).

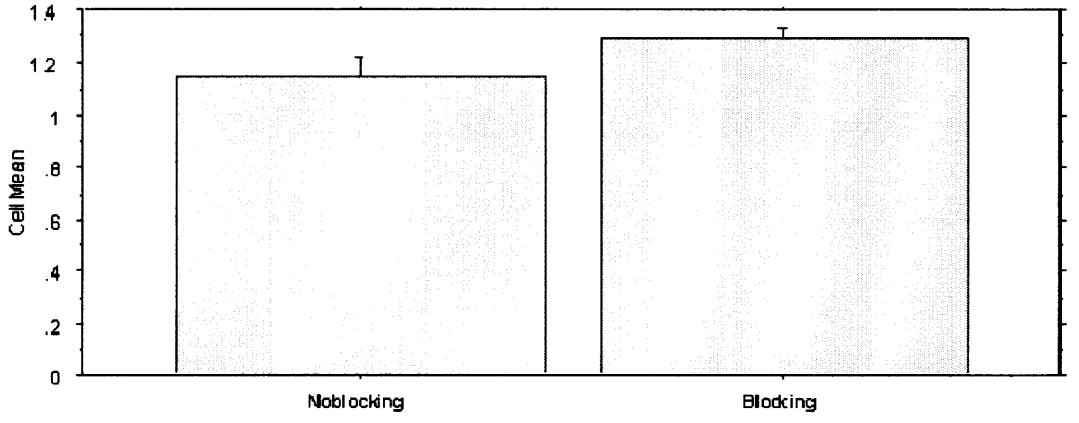

Figure 4.22 Bar plot for average deviation area versus the type of haptics delivered. (No blocking mean area = 1.153, blocking mean area = 1.294) (Error bars: ± standard error)

There is no statistical significance between each learning set and the deviation area ($F(4, 16) = 1.247$, $p = 0.3308$). As the test trials progress, the average deviation area generally increases.

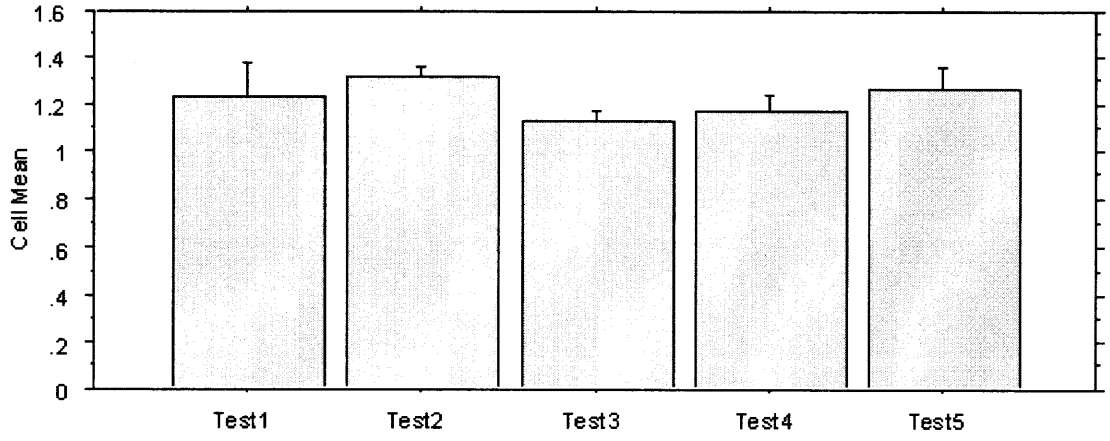

Figure 4.23 Bar plot for average deviation area versus each of the five test sets. Both forms of haptics are included in this evaluation. (Test 1 = 1.229, test 2 = 1.314, test 3 = 1.133, test 4 = 1.171, test 5 = 1.270) (Error bars: ± standard error)

Subject 3 also does not show any learning with the presence of blocking haptic feedback and shows a slight decrease in the average deviation area with no blocking feedback received. These results are statistically significant ($F(4, 4) = 4.566$, $p = 0.0119$).

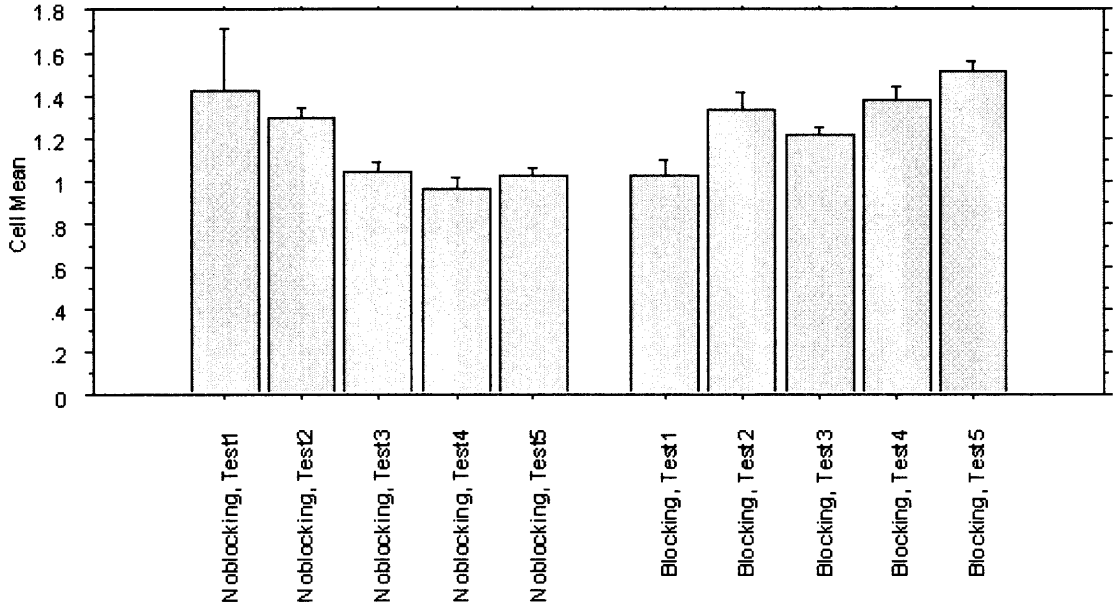

Figure 4.24 Bar plot for average deviation area versus each of the five test sets with respect to the type of haptic feedback delivered. (Error bars: ± standard error)

4.2.5 Linear Trajectory: Movement Duration

Using ANOVA to analyze any changes or variations in the time required for the subjects to complete test trials in the linear trajectory produces results which are not statistically significant. When comparing the time required to complete the trajectory with the type of haptic feedback delivered the results are what was expected. As shown in figure 4.25, no blocking haptic feedback allows the subjects to complete the trajectory more rapidly than blocking feedback. However, these results are not statistically significant ($F(1, 2) = 16.320$, $p = 0.0562$).

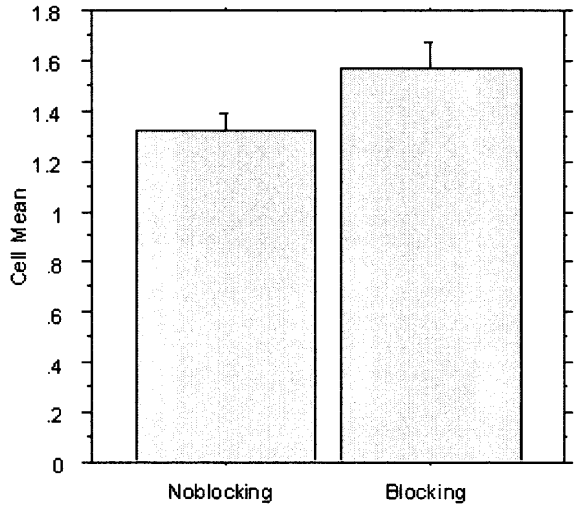

Figure 4.25 Bar plot for duration time versus the type of haptics delivered. (No blocking mean area = 1.322, blocking mean area = 1.569) (Error bars: ± standard error)

There is also no statistical significance when comparing the amount of time required to complete the trajectory to the test set number ($F(4, 2) = 1.895$, $p = 0.2048$). However, it is seen that the amount of time required to complete the trajectory does slightly decrease throughout the experiments regardless of the type of haptic feedback delivered.

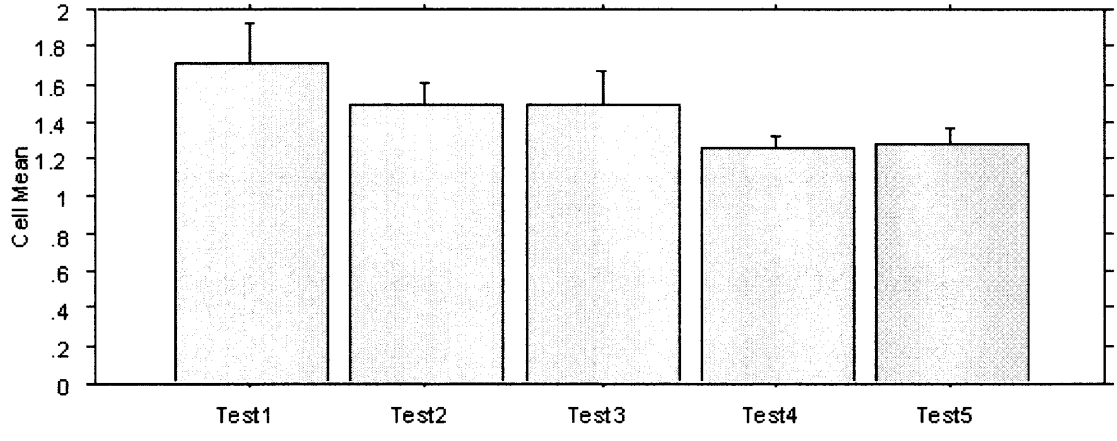

Figure 4.26 Bar plot for duration time versus each of the five test sets. Both forms of haptics are included in this evaluation. (Test 1 = 1.715, test 2 = 1.489, test 3 = 1.489, test 4 = 1.258, test 5 = 1.275) (Error bars: ± standard error)

There is no significant haptic feedback x test set interaction ($F(4, 16) = 0.882$, $p = 0.5158$). In figure 4.27, it is shown that while the duration time from the first to the fifth test set does decrease with both types of haptic feedback present, it is not a steady or consistent decline in either case.

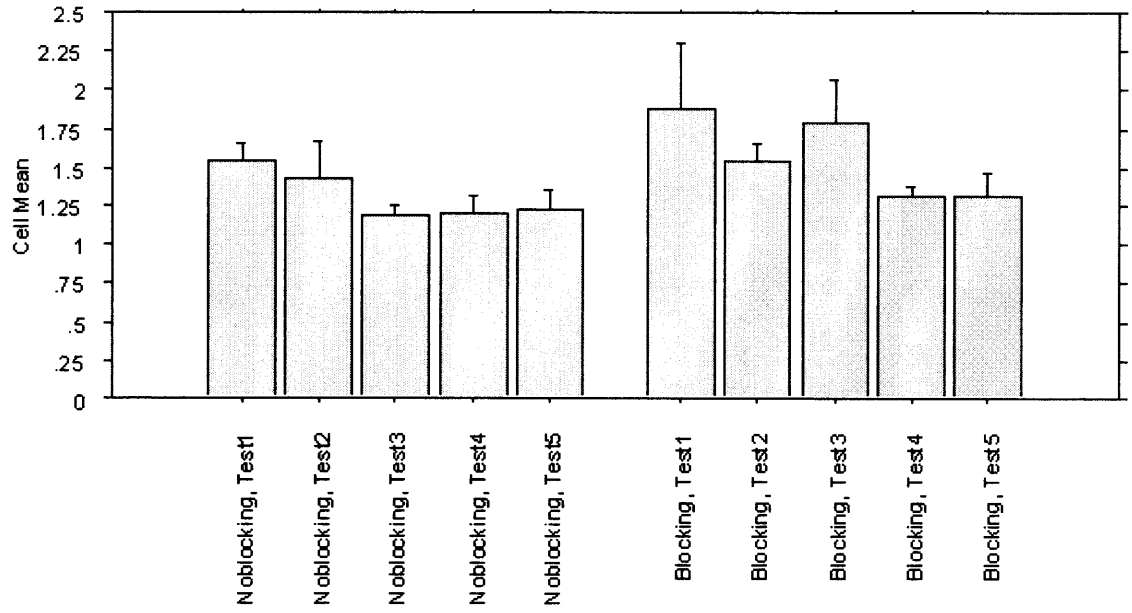

Figure 4.27 Bar plot for duration time versus each of the five test sets with respect to the type of haptic feedback delivered. (Error bars: ± standard error)

CHAPTER 5

DISCUSSION AND FUTURE WORK

5.1 Discussion

Several conclusions may be drawn from the results of this research. A primary result seen is that a higher degree of learning occurs within the cube maze when no blocking force feedback is received than blocking force feedback. The subjects had an easier time smoothly following the optimum trajectory and maneuvering through the environment in this situation, which seemingly allowed for them to learn the trajectory at a more efficient rate. No blocking feedback allowed them to more closely follow the shape of the desired trajectory because the sphere was permitted to travel along the walls of the cubes. They also reported enjoying the activity more and became less frustrated with the no blocking feedback than with the blocking feedback. During blocking feedback, when the sphere hit the cube walls the force vector had to be redirected towards the optimal trajectory to continue movement. Therefore, it was not as easy for the subject to smoothly follow the optimum trajectory.

Within the linear trajectory environment, no blocking feedback also induced a higher degree of learning than blocking feedback in two thirds of the subjects. Virtual environments with varying complexity levels may require different haptic feedback to bring about motor learning. However, despite the difference in the two environments and the number of turns required in the cube maze compared to the lack of turns in the trajectory, no blocking haptic feedback was still more efficient in promoting learning in the subjects.

Another conclusion that can be drawn from this research is that although the presence of visual feedback was expected to cause a dramatically decreased deviation area, it did not and when a decreased are resulted, it was not statistically significant. There was no significant visual feedback x haptic feedback interaction and there was also no significant visual feedback x test number interaction effect. Since visual feedback allowed the subject to follow the optimal trajectory with the sphere, which added a second component of feedback, it was expected to produce improved results compared to when it was not present. It was also believed that the subject would be able to maintain increased levels of concentration and attention with the inclusion of visual feedback and this would therefore lead to an increased ability for them to follow the optimal trajectory.

In the cube maze and linear trajectory environment, the movement duration during the testing trials was faster with the no blocking feedback condition. As the test sets continued, there was a slight decrease in the time required to complete the test trials. During the cube maze environment, the presence of vision did not effect the movement duration time. From these results, we can hypothesize that the learning that occurred was motor learning and not cognitive learning. It is expected that cognitive learning would cause the subjects to maneuver through the virtual environments at a slower speed to avoid friction caused by contact with the cube and side walls.

A main limitation to increased motor learning through this activity is shoulder fatigue. It was reported by all of the subjects that towards the end of each experiment session their shoulder was fatigued. During the fifth testing set, they often showed poorer results than from prior testing sets. The subjects reported that the continuous and repetitive motion involved in the experiments caused their shoulder to tire.

A final aspect that is gathered from this study involves the amount of time that learning is retained due to the experimentation. Certain portions of these results suggest that learning is only short term, and may last approximately 24 hours or less. In the cube maze with visual feedback, it is seen that subject 1 retains some memory of the desired trajectory from one day to the next due to the fact that there is a higher degree of learning the second day of training, despite the presence of blocking feedback. The other subjects completed the no blocking force feedback scenario three days prior to the blocking force feedback and showed no signs of retaining any memory of the maze or the desired motion to mimic the optimal trajectory.

5.2 Future Work

There are several possibilities for future work in this area of research. Different support systems may be worn by the subject during testing. An arm support system or brace may be utilized in order to reduce the subject's shoulder fatigue. The support system can be hung from the ceiling or attached to the floor or chair. Reducing shoulder fatigue would be extremely helpful in allowing the subject to undergo longer durations of training sessions and would therefore further the benefits of the training. A torso brace may be worn, which would secure the subject's body to the chair. Having this additional support system would restrict movement from areas of the body other than the shoulder and arm. This would allow for heightened improvements from the activity and would also produce more accurate data due to the limiting of movement from other areas of the body.

Another possibility of future work would be to wear the CyberGlove to train finger motion in conjunction with the training of arm and shoulder movement via the

Haptic Master. Stereo goggles may also be worn to create a three dimensional environment for the subject to maneuver throughout.

Also, it is a future possibility to create more advanced virtual environments for subjects to experience. This would generate more interest from the patients, maintaining their attention during additional experimental sessions, leading to potentially increased motor learning. With more environments, it is a possibility to compare different environments and whether learning is generalized to a specific condition. For example, if a subject learns one orientation it can be determined if it is easier to learn a different orientation. Or, it can be determined if it is easier to learn with or without stereo goggles.

Finally, in the future, stroke patients can become involved in this type of study rather than having subjects with no history of motor disorders. This would allow for the determination of the actual benefits of this type of activity to patients with disabilities.

APPENDIX A MATLAB CODE: DEVIATION AREA

This appendix includes the Matlab code used to calculate the difference in area between the optimal trajectory and each trial's trajectory.

```
%Calculate the Deviation Between the Optimal and Trial Trajectories: Area

AA=input('What is the name of the file you want to load?\n', 's')
SF=100; %Sampling Frequency;
Path1=pwd; C=[]; Cump=[]; Dur=[]; Smooth=[]; Area1=[];
Filename=[Path1 '\' AA];
if (~isempty(Filename))
  C=load(Filename);
end

%define trials
[rows,cols]=size(C);
count=0; newi=1;
for i=2:rows
  if(C(i,cols)~=C(i-1,cols))
    count=count+1;
    t{count}=C(newi:i-1,:);
    newi=i;
  end
end
count=count+1;
t{count}=C(newi:i,:);

for i=1:size(t,2)
  C=t{i};          %C=t{1}, C=t{2}...;
  [rows,cols]=size(C);


  %Assume Data from One Trial is Saved in Matrix C

  %Optimal Trajectory

  P1=[0.0096, 0.0096, 0.0096, 0.0096, 0.0096, 0.0096];
  P2=[-0.0325, -0.0325, 0.0325, 0.0325, -0.0325, -0.0325];
  P3=[-0.205, -0.135, -0.135, -0.05, -0.05, 0.025];

  figure(2)
  plot3(P1, P2, P3, 'r')
  grid
```

```
az=90;
el=0;
view(az, el);
xlabel('X Trajectory')
ylabel('Y Trajectory')
zlabel('Z Trajectory')

hold on

%This Program Calculates the Deviation between the Actual and Optimal Trajectory

%First step: Find All Cross Points Between Two Trajectories

point_num=size(C);
cross_num=1;

cross(1,1:3)=C(1,2:4);
cross(1,4)=1;
cross(1,5)=1;

%Format of Matrix Cross is Following: (X, Y, Z, line#, point_num)

for i=1:point_num(1)-1
  if ( (C(i,3)-P2(1))* (C(i+1,3)-P2(1))<=0 ) %if point on the line :Y=Y1
    if C(i,4)<=P3(2)
      cross_num=cross_num+1;
      cross(cross_num,1:3)=C(i,2:4);
      cross(cross_num,4)=1;
      cross(cross_num,5)=i;
    else
      if C(i,4)>=P3(5)
        cross_num=cross_num+1;
        cross(cross_num,1:3)=C(i,2:4);
        cross(cross_num,4)=5;
        cross(cross_num,5)=i;
      end
    end
  else
    if ( (C(i,3)-P2(3))*(C(i+1,3)-P2(3))<=0)
      if ( (C(i,4)<=P3(5)) && (C(i,4)>=P3(2)))
        cross_num=cross_num+1;
        cross(cross_num,1:3)=C(i,2:4);
        cross(cross_num,4)=3;
        cross(cross_num,5)=i;
      end
    else
```

```
        if ( (C(i,4)-P3(2)) * (C(i+1,4)-P3(2)) <=0)
           cross_num=cross_num+1;
           cross(cross_num,1:3)=C(i,2:4);
           cross(cross_num,4)=2;
           cross(cross_num,5)=i;
        else
           if ( (C(i,4)-P3(5))*(C(i+1,4)-P3(5))<=0)
              cross_num=cross_num+1;
              cross(cross_num,1:3)=C(i,2:4);
              cross(cross_num,4)=4;
              cross(cross_num,5)=i;
           end
        end
     end
  end
end

%Calculate the Deviation Area

area=0;

for i=1:cross_num-1
  switch cross(i,4)
     case 1,
        switch cross(i+1,4)
           case {1,2}
              for j=cross(i,5):cross(i+1,5)
                 area=area+abs(C(j,3)-P2(1));
                 plot3([P1(1) P1(1)],[C(j,3) P2(1)],[C(j,4) C(j,4)]);
                 hold on
              end
           case {3,4}
              for j=cross(i,5):cross(i+1,5)
                 if (C(j,4)<=P3(2))
                    area=area+abs(C(j,3)-P2(1));
                    plot3([P1(1) P1(1)],[C(j,3) P2(1)],[C(j,4) C(j,4)]);
                    hold on
                 else
                    area=area+abs(C(j,3)-P2(3));
                    plot3([P1(1) P1(1)],[C(j,3) P2(3)],[C(j,4) C(j,4)]);
                    hold on
                 end
              end
           case 5,
              for j=cross(i,5):cross(i+1,5)
                 if ((C(j,4)<=P3(2)) && (C(j,4)>=P3(2)))
```

```
            area=area+abs(C(j,3)-P2(1));
            plot3([P1(1) P1(1)],[C(j,3) P2(1)],[C(j,4) C(j,4)]);
            hold on
          else
            area=area+abs(C(j,3)-P2(3));
            plot3([P1(1) P1(1)],[C(j,3) P2(3)],[C(j,4) C(j,4)]);
            hold on
          end
        end
    end
case 2,
    switch cross(i+1,4)
      case 2,
        for j=cross(i,5):cross(i+1,5)
          area=area+abs(C(j,4)-P3(2));
          plot3([P1(1) P1(1)],[C(j,3) C(j,3)],[C(j,4) P3(2)]);
          hold on
        end
      case {3,4}
        for j=cross(i,5):cross(i+1,5)
          area=area+abs(C(j,3)-P2(3));
          plot3([P1(1) P1(1)],[C(j,3) P2(3)],[C(j,4) C(j,4)]);
          hold on
        end
      case 5,
        for j=cross(i,5):cross(i+1,5)
          if (C(j,4)>=P3(5))
            area=area+abs(C(j,3)-P2(1));
            plot3([P1(1) P1(1)],[C(j,3) P2(1)],[C(j,4) C(j,4)]);
            hold on
          else
            area=area+abs(C(j,3)-P2(3));
            plot3([P1(1) P1(1)],[C(j,3) P2(3)],[C(j,4) C(j,4)]);
            hold on
          end
        end
    end
case 3,
    switch cross(i+1,4)
      case {3,4}
        for j=cross(i,5):cross(i+1,5)
          area=area+abs(C(j,3)-P2(3));
          plot3([P1(1) P1(1)],[C(j,3) P2(3)],[C(j,4) C(j,4)]);
          hold on
        end
      case 5,
```

```
                for j=cross(i,5):cross(i+1,5)
                    if (C(j,4)>=P3(5))
                        area=area+abs(C(j,3)-P2(1));
                        plot3([P1(1) P1(1)],[C(j,3) P2(1)],[C(j,4) C(j,4)]);
                        hold on
                    else
                        area=area+abs(C(j,3)-P2(3));
                        plot3([P1(1) P1(1)],[C(j,3) P2(3)],[C(j,4) C(j,4)]);
                        hold on
                    end
                end
            end
        case 4,
            switch cross(i+1,4)
                case 4,
                    for j=cross(i,5):cross(i+1,5)
                        area=area+abs(C(j,4)-P3(5));
                        plot3([P1(1) P1(1)],[C(j,3) C(j,3)],[C(j,4) P3(5)]);
                        hold on
                    end
                case 5,
                    for j=cross(i,5):cross(i+1,5)
                        area=area+abs(C(j,3)-P2(1));
                        plot3([P1(1) P1(1)],[C(j,3) P2(1)],[C(j,4) C(j,4)]);
                        hold on
                    end
            end
        case 5,
            for j=cross(i,5):cross(i+1,5)
                area=area+abs(C(j,3)-P2(1));
                plot3([P1(1) P1(1)],[C(j,3) P2(1)],[C(j,4) C(j,4)]);
                hold on
            end
    end
end

if (cross(i+1,5)<point_num(1))
    for k=cross(i+1,5):point_num(1)
        if C(k,4)<=P3(2)
            area=area+abs(C(k,3)-P2(1))
            plot3([P1(1) P1(1)],[C(k,3) P2(1)],[C(k,4) C(k,4)]);
            hold on
        else
            if C(k,4)<=P3(5)
                area=area+abs(C(k,3)-P2(3));
                plot3([P1(1) P1(1)],[C(k,3) P2(3)],[C(k,4) C(k,4)]);
```

```
            hold on
          else
            if C(k,4)>P3(5)
              %'asdf'
              area=area+abs(C(k,3)-P2(1))
              plot3([P1(1) P1(1)],[C(k,3) P2(1)],[C(k,4) C(k,4)],'b');
              hold on
            end
          end
        end
      end
    end

    Area1=[Area1,area]
    clear t{i}
end

%Save Deviation Areas

save ('Area1')

%Plot Deviation Areas vs. Trial

figure(3)
plot(Area1, 'r')
ZZ=get(gca,'YLim')
line([5,5],ZZ);      %mark experimental stages
line([20,20],ZZ);
line([25,25],ZZ);
line([40,40],ZZ);
line([45,45],ZZ);
line([60,60],ZZ);
line([65,65],ZZ);
line([80,80],ZZ);

%Calculate the Deviation Between the Optimal and Trial Straight Trajectories: Area

AA=input('What is the name of the file you want to load?\n', 's')
SF=100; %Sampling Frequency;
Path1=pwd; C=[]; Cump=[]; Dur=[]; Smooth=[]; Area1=[];
Filename=[Path1 '\' AA];
if (~isempty(Filename))
  C=load(Filename);
end

%define trials
```

```
[rows,cols]=size(C);
count=0; newi=1;
for i=2:rows
   if(C(i,cols)~=C(i-1,cols))
      count=count+1;
      t{count}=C(newi:i-1,:);
      newi=i;
   end
end
count=count+1;
t{count}=C(newi:i,:);

for i=1:size(t,2)
   C=t{i};            %C=t{1}, C=t{2}...;
   [rows,cols]=size(C);

   area=0;

   for j=1:rows
      area=area+abs(C(j,2));
   end

   Area1=[Area1,area]

   %Optimal Trajectory

   P2=[0.0096, 0.0096];
   P1=[0, 0];
   P3=[-0.205, 0.025];

   figure(2)
   plot3(P1, P2, P3, 'r')
   grid
   az=90;
   el=0;
   view(az, el);
   xlabel('X Trajectory')
   ylabel('Y Trajectory')
   zlabel('Z Trajectory')

   hold on

end

clear t{i}
```

APPENDIX B MATLAB CODE: PLOT AVERAGE AND STANDARD DEVIATION

In this appendix, the Matlab code is shown that was used to plot the average and standard deviation for each learning set of five trials.

```
%Find Area for Each Group of 5
A1=mean(Area1(1:5));
A2=mean(Area1(21:25));
A3=mean(Area1(41:45));
A4=mean(Area1(61:65));
A5=mean(Area1(81:85));

%Find Standard Deviation for Each Group of 5
S1=std(Area1(1:5));
S2=std(Area1(21:25));
S3=std(Area1(41:45));
S4=std(Area1(61:65));
S5=std(Area1(81:85));

%Plot Avgs and Std Dev
figure(4)
plot(1,A1,'--ro')
hold on
plot(2,A2,'--ro')
plot(3,A3,'--ro')
plot(4,A4,'--ro')
plot(5,A5,'--ro')

plot(1,A1+S1,'bo')
plot(1,A1-S1,'bo')
plot(2,A2+S2,'bo')
plot(2,A2-S2,'bo')
plot(3,A3+S3,'bo')
plot(3,A3-S3,'bo')
plot(4,A4+S4,'bo')
plot(4,A4-S4,'bo')
plot(5,A5+S5,'bo')
plot(5,A5-S5,'bo')

xlabel('Set of Five')
ylabel('Area')
```

APPENDIX C MATLAB CODE: CUMULATIVE PATH, MOVEMENT DURATION, AND SMOOTHNESS

This appendix includes the Matlab code used to calculate the cumulative path, the movement duration, and the smoothness of each trial's trajectory.

```
AA=input('What is the name of the file you want to load?\n', 's')
SF=100; %Sampling Frequency
Path1=pwd; C=[]; Cump=[]; Dur=[]; Smooth=[];
Filename=[Path1 '\' AA];
if (~isempty(Filename))
   C=load(Filename);
end

%define trials
[rows,cols]=size(C);
count=0; newi=1;
for i=2:rows
   if(C(i,cols)>C(i-1,cols))
      count=count+1;
      t{count}=C(newi:i-1,:);
      newi=i;
   end
end
count=count+1;
t{count}=C(newi:i,:);

for i=1:size(t,2)
   C=t{i};
   [rows,cols]=size(C);

   %Define Time and X,Y,Z Position, Velocity, Acceleration
   Time=C(:,1);
   Xp=C(:,2);
   Yp=C(:,3);
   Zp=C(:,4);
   Xv=C(:,5);
   Yv=C(:,6);
   Zv=C(:,7);
   Xf=C(:,8);
   Yf=C(:,9);
   Zf=C(:,10);

   %Filter Position Data
```

```
[B,A]=butter(2, 0.2);
Xp_filt=filter(B,A,Xp);
Yp_filt=filter(B,A,Yp);
Zp_filt=filter(B,A,Zp);

xx=1:10:rows;

%Function
dt=diff(Time);
Ix=integrfixed(Xp_filt, dt);

N=length(Xp_filt);
Ix=0;
for(i=1:N-1)
   Ix=Ix+dt*(Xp_filt(i)+0.5*(Xp_filt(i)-Xp_filt(i+1)));
end

%Smoothness of Trajectory
%Tangential Velocity
TangVel=sqrt(Xv.^2+Yv.^2+Zv.^2);

%Calculate Acceleration
AccX=diff(Xv);
AccY=diff(Yv);
AccZ=diff(Zv);

%Tangential Acceleration
TangAcc=sqrt(AccX.^2+AccY.^2+AccZ.^2);

%Jerk=Derivative of Acceleration
JerkX=diff(AccX);
JerkY=diff(AccY);
JerkZ=diff(AccZ);

%Jerk Squared
JerkX_2=(JerkX.^2);
JerkY_2=(JerkY.^2);
JerkZ_2=(JerkZ.^2);

% Tangential Jerk
TangJerk=sqrt(JerkX_2.^2+JerkY_2.^2+JerkZ_2.^2);

%Tangential Jerk Squared
TangJerk_2=TangJerk.^2;

%Smoothness=Integral of Jerk Squared
```

```
   Smoothness=integrfixed(TangJerk, 1/SF)

   %Calculate Trajectory Length
   for n=1:length(Xp_filt)-1
      A(n)=sqrt((Xp_filt(n+1)-Xp_filt(n))^2+(Yp_filt(n+1)-Yp_filt(n))^2+(Zp_filt(n+1)-
Zp_filt(n))^2);
   end

   for n=2:length(Xp_filt)-1
      A(n)=A(n-1) + A(n);
   end

   A=[A(1); A'];
   Cumpath=A(length(Xp_filt))

   % Calculate Movement Duration
   Duration=(1/SF)*(length(Xp_filt)-2)

   Cump=[Cump,Cumpath];
   Dur=[Dur,Duration];
   Smooth=[Smooth,Smoothness];

end

%Save Parameters

save ('Amanda', 'Cump', 'Dur', 'Smooth')

%Plot Cump, Dur, Smooth

figure(1)
subplot(1,3,1);
plot(Cump, 'r.')
grid on
axis tight
xlabel('Trial')
ylabel('Cump')
hold on
ZZ=get(gca,'YLim')
line([5,5],ZZ);      %mark experimental stages
line([20,20],ZZ);
line([25,25],ZZ);
line([40,40],ZZ);
line([45,45],ZZ);
line([60,60],ZZ);
line([65,65],ZZ);
```

```
line([80,80],ZZ);

subplot(1,3,2);
plot(Dur, 'r.')
grid on
axis tight
xlabel('Trial')
ylabel('Dur')
hold on
ZZ=get(gca,'YLim')
line([5,5],ZZ);      %mark experimental stages
line([20,20],ZZ);
line([25,25],ZZ);
line([40,40],ZZ);
line([45,45],ZZ);
line([60,60],ZZ);
line([65,65],ZZ);
line([80,80],ZZ);

subplot (1,3,3);
plot(Smooth, 'r.')
grid on
axis tight
xlabel('Trial')
ylabel('Smooth')
hold on
ZZ=get(gca,'YLim')
line([5,5],ZZ);      %mark experimental stages
line([20,20],ZZ);
line([25,25],ZZ);
line([40,40],ZZ);
line([45,45],ZZ);
line([60,60],ZZ);
line([65,65],ZZ);
line([80,80],ZZ);
```

APPENDIX D MATLAB CODE: PLOT TRAJECTORIES

In this appendix, the Matlab code that was used to plot trajectories is shown.

```
%Optimal Trajectory

P1=[0.0096, 0.0096, 0.0096, 0.0096, 0.0096, 0.0096];
P2=[-0.0325, -0.0325, 0.0325, 0.0325, -0.0325, -0.0325];
P3=[-0.205, -0.135, -0.135, -0.05, -0.05, 0.025];

%First Five

NoHaptics1=input('What is the name of the file you want to load?\n', 's')
Path1=pwd; S1=[];
Filename=[Path1 '\' NoHaptics1];
if (~isempty(Filename))
   S1=load(Filename);
end

%Define Trials

[rows,cols]=size(S1);
count=0; newi=1;
for i=2:rows
   if(S1(i,cols)>S1(i-1,cols))
      count=count+1;
      t1{count}=S1(newi:i-1,:);
      newi=i;
   end
end
count=count+1;
t1{count}=S1(newi:i,:);

for i=1:size(t1,2)
   S1=t1{i};
   [rows,cols]=size(S1);

   %Define Time and X,Y,Z Position, Velocity, Acceleration

   Time_S1_1=S1(:,1);
   Xp_S1_5=S1(:,2);
   Yp_S1_5=S1(:,3);
   Zp_S1_5=S1(:,4);
   Xv_S1_5=S1(:,5);
```

```
   Yv_S1_5=S1(:,6);
   Zv_S1_5=S1(:,7);
   Xf_S1_5=S1(:,8);
   Yf_S1_5=S1(:,9);
   Zf_S1_5=S1(:,10);

   %Plot First Five With Optimal Traj

   figure(4)
   subplot(2,4,1)
   plot3(P1, P2, P3, 'r','LineWidth',4)
   grid
   az=90;
   el=0;
   view(az, el);
   xlabel('X Trajectory')
   ylabel('Y Trajectory')
   zlabel('Z Trajectory')

   hold on

   plot3(Xp_S1_5, Yp_S1_5, Zp_S1_5)
   grid
   az=90;
   el=0;
   view(az, el);
   xlabel('X Trajectory')
   ylabel('Y Trajectory')
   zlabel('Z Trajectory')
   title('First Five: No Haptics')

end

%Second Fifteen

Haptics2=input('What is the name of the file you want to load?\n', 's')
Path1=pwd; S2=[];
Filename=[Path1 '\' Haptics2];
if (~isempty(Filename))
   S2=load(Filename);
end

%Define Trials

[rows,cols]=size(S2);
count=0; newi=1;
```

```
for i=2:rows
   if(S2(i,cols)>S2(i-1,cols))
      count=count+1;
      t2{count}=S2(newi:i-1,:);
      newi=i;
   end
end
count=count+1;
t2{count}=S2(newi:i,:);

for i=1:size(t2,2)
   S2=t2{i};
   [rows,cols]=size(S2);

   %Define Time and X,Y,Z Position, Velocity, Acceleration

   Time_S2_15=S2(:,1);
   Xp_S2_15=S2(:,2);
   Yp_S2_15=S2(:,3);
   Zp_S2_15=S2(:,4);
   Xv_S2_15=S2(:,5);
   Yv_S2_15=S2(:,6);
   Zv_S2_15=S2(:,7);
   Xf_S2_15=S2(:,8);
   Yf_S2_15=S2(:,9);
   Zf_S2_15=S2(:,10);

   %Plot Second Fifteen With Optimal Traj

   subplot(2,4,2)
   plot3(P1, P2, P3, 'r','LineWidth',4)
   grid
   az=90;
   el=0;
   view(az, el);
   xlabel('X Trajectory')
   ylabel('Y Trajectory')
   zlabel('Z Trajectory')

   hold on

   plot3(Xp_S2_15, Yp_S2_15, Zp_S2_15)
   grid
   az=90;
   el=0;
   view(az, el);
```

```
   xlabel('X Trajectory')
   ylabel('Y Trajectory')
   zlabel('Z Trajectory')
   title('Second Fifteen: Haptics')

end

%Third Five

NoHaptics3=input('What is the name of the file you want to load?\n', 's')
Path=pwd; S3=[];
Filename=[Path1 '\' NoHaptics3];
if (~isempty(Filename))
   S3=load(Filename);
end

%Define Trials

[rows,cols]=size(S3);
count=0; newi=1;
for i=2:rows
   if(S3(i,cols)>S3(i-1,cols))
      count=count+1;
      t3{count}=S3(newi:i-1,:);
      newi=i;
   end
end
count=count+1;
t3{count}=S3(newi:i,:);

for i=1:size(t3,2)
   S3=t3{i};
   [rows,cols]=size(S3);

   %Define Time and X,Y,Z Position, Velocity, Acceleration

   Time_S3_5=S3(:,1);
   Xp_S3_5=S3(:,2);
   Yp_S3_5=S3(:,3);
   Zp_S3_5=S3(:,4);
   Xv_S3_5=S3(:,5);
   Yv_S3_5=S3(:,6);
   Zv_S3_5=S3(:,7);
   Xf_S3_5=S3(:,8);
   Yf_S3_5=S3(:,9);
   Zf_S3_5=S3(:,10);
```

```
   %Plot Third Five With Optimal Traj

   subplot(2,4,3)
   plot3(P1, P2, P3, 'r','LineWidth',4)
   grid
   az=90;
   el=0;
   view(az, el);
   xlabel('X Trajectory')
   ylabel('Y Trajectory')
   zlabel('Z Trajectory')

   hold on

   plot3(Xp_S3_5, Yp_S3_5, Zp_S3_5)
   grid
   az=90;
   el=0;
   view(az, el);
   xlabel('X Trajectory')
   ylabel('Y Trajectory')
   zlabel('Z Trajectory')
   title('Third Five: No Haptics')

end

%Fourth Fifteen

Haptics4=input('What is the name of the file you want to load?\n', 's')
Path1=pwd; S4=[];
Filename=[Path1 '\' Haptics4];
if (~isempty(Filename))
   S4=load(Filename);
end

%Define Trials

[rows,cols]=size(S4);
count=0; newi=1;
for i=2:rows
   if(S4(i,cols)>S4(i-1,cols))
      count=count+1;
      t3{count}=S4(newi:i-1,:);
      newi=i;
   end
```

```
end
count=count+1;
t3{count}=S4(newi:i,:);

for i=1:size(t3,2)
   S4=t3{i};
   [rows,cols]=size(S4);

   %Define Time and X,Y,Z Position, Velocity, Acceleration

   Time_S4_15=S4(:,1);
   Xp_S4_15=S4(:,2);
   Yp_S4_15=S4(:,3);
   Zp_S4_15=S4(:,4);
   Xv_S4_15=S4(:,5);
   Yv_S4_15=S4(:,6);
   Zv_S4_15=S4(:,7);
   Xf_S4_15=S4(:,8);
   Yf_S4_15=S4(:,9);
   Zf_S4_15=S4(:,10);

   %Plot Fourth Fifteen With Optimal Traj

   subplot(2,4,4)
   plot3(P1, P2, P3, 'r','LineWidth',4)
   grid
   az=90;
   el=0;
   view(az, el);
   xlabel('X Trajectory')
   ylabel('Y Trajectory')
   zlabel('Z Trajectory')

   hold on

   plot3(Xp_S4_15, Yp_S4_15, Zp_S4_15)
   grid
   az=90;
   el=0;
   view(az, el);
   xlabel('X Trajectory')
   ylabel('Y Trajectory')
   zlabel('Z Trajectory')
   title('Fourth Fifteen: Haptics')

end
```

```
%Fifth Five

NoHaptics5=input('What is the name of the file you want to load?\n', 's')
Path1=pwd; S5=[];
Filename=[Path1 '\' NoHaptics5];
if (~isempty(Filename))
   S5=load(Filename);
end

%Define Trials

[rows,cols]=size(S5);
count=0; newi=1;
for i=2:rows
   if(S5(i,cols)>S5(i-1,cols))
      count=count+1;
      t3{count}=S5(newi:i-1,:);
      newi=i;
   end
end
count=count+1;
t3{count}=S5(newi:i,:);

for i=1:size(t3,2)
   S5=t3{i};
   [rows,cols]=size(S5);

   %Define Time and X,Y,Z Position, Velocity, Acceleration

   Time_S5_5=S5(:,1);
   Xp_S5_5=S5(:,2);
   Yp_S5_5=S5(:,3);
   Zp_S5_5=S5(:,4);
   Xv_S5_5=S5(:,5);
   Yv_S5_5=S5(:,6);
   Zv_S5_5=S5(:,7);
   Xf_S5_5=S5(:,8);
   Yf_S5_5=S5(:,9);
   Zf_S5_5=S5(:,10);

   %Plot Fifth Five With Optimal Traj

   subplot(2,4,5)
   plot3(P1, P2, P3, 'r','LineWidth',4)
   grid
```

```
   az=90;
   el=0;
   view(az, el);
   xlabel('X Trajectory')
   ylabel('Y Trajectory')
   zlabel('Z Trajectory')

   hold on

   plot3(Xp_S5_5, Yp_S5_5, Zp_S5_5)
   grid
   az=90;
   el=0;
   view(az, el);
   xlabel('X Trajectory')
   ylabel('Y Trajectory')
   zlabel('Z Trajectory')
   title('Fifth Five: No Haptics')

end

%Sixth Fifteen

Haptics15=input('What is the name of the file you want to load?\n', 's')
Path1=pwd; S6=[];
Filename=[Path1 '\' Haptics15];
if (~isempty(Filename))
   S6=load(Filename);
end

%Define Trials

[rows,cols]=size(S6);
count=0; newi=1;
for i=2:rows
   if(S6(i,cols)>S6(i-1,cols))
      count=count+1;
      t3{count}=S6(newi:i-1,:);
      newi=i;
   end
end
count=count+1;
t3{count}=S6(newi:i,:);

for i=1:size(t3,2)
   S6=t3{i};
```

```
[rows,cols]=size(S6);

%Define Time and X,Y,Z Position, Velocity, Acceleration

Time_S6_15=S6(:,1);
Xp_S6_15=S6(:,2);
Yp_S6_15=S6(:,3);
Zp_S6_15=S6(:,4);
Xv_S6_15=S6(:,5);
Yv_S6_15=S6(:,6);
Zv_S6_15=S6(:,7);
Xf_S6_15=S6(:,8);
Yf_S6_15=S6(:,9);
Zf_S6_15=S6(:,10);

%Plot Sixth Fifteen With Optimal Traj

subplot(2,4,6)
plot3(P1, P2, P3, 'r','LineWidth',4)
grid
az=90;
el=0;
view(az, el);
xlabel('X Trajectory')
ylabel('Y Trajectory')
zlabel('Z Trajectory')

hold on

plot3(Xp_S6_15, Yp_S6_15, Zp_S6_15)
grid
az=90;
el=0;
view(az, el);
xlabel('X Trajectory')
ylabel('Y Trajectory')
zlabel('Z Trajectory')
title('Sixth Fifteen: Haptics')

end

%Seventh Five

NoHaptics7=input('What is the name of the file you want to load?\n', 's')
Path1=pwd; S7=[];
Filename=[Path1 '\' NoHaptics7];
```

```
if (~isempty(Filename))
   S7=load(Filename);
end

%Define Trials

[rows,cols]=size(S7);
count=0; newi=1;
for i=2:rows
   if(S7(i,cols)>S7(i-1,cols))
      count=count+1;
      t3{count}=S7(newi:i-1,:);
      newi=i;
   end
end
count=count+1;
t3{count}=S7(newi:i,:);

for i=1:size(t3,2)
   S7=t3{i};
   [rows,cols]=size(S7);

   %Define Time and X,Y,Z Position, Velocity, Acceleration

   Time_S7_5=S7(:,1);
   Xp_S7_5=S7(:,2);
   Yp_S7_5=S7(:,3);
   Zp_S7_5=S7(:,4);
   Xv_S7_5=S7(:,5);
   Yv_S7_5=S7(:,6);
   Zv_S7_5=S7(:,7);
   Xf_S7_5=S7(:,8);
   Yf_S7_5=S7(:,9);
   Zf_S7_5=S7(:,10);

   %Plot Seventh Five With Optimal Traj

   subplot(2,4,7)
   plot3(P1, P2, P3, 'r','LineWidth',4)
   grid
   az=90;
   el=0;
   view(az, el);
   xlabel('X Trajectory')
   ylabel('Y Trajectory')
   zlabel('Z Trajectory')
```

```
   hold on

   plot3(Xp_S7_5, Yp_S7_5, Zp_S7_5)
   grid
   az=90;
   el=0;
   view(az, el);
   xlabel('X Trajectory')
   ylabel('Y Trajectory')
   zlabel('Z Trajectory')
   title('Seventh Five: No Haptics')

end

%Eighth Fifteen

Haptics15=input('What is the name of the file you want to load?\n', 's')
Path1=pwd; S8=[];
Filename=[Path1 '\' Haptics15];
if (~isempty(Filename))
   S8=load(Filename);
end

%Define Trials

[rows,cols]=size(S8);
count=0; newi=1;
for i=2:rows
   if(S8(i,cols)>S8(i-1,cols))
      count=count+1;
      t3{count}=S8(newi:i-1,:);
      newi=i;
   end
end
count=count+1;
t3{count}=S8(newi:i,:);

for i=1:size(t3,2)
   S8=t3{i};
   [rows,cols]=size(S8);

   %Define Time and X,Y,Z Position, Velocity, Acceleration

   Time_S8_15=S8(:,1);
   Xp_S8_15=S8(:,2);
```

```
Yp_S8_15=S8(:,3);
Zp_S8_15=S8(:,4);
Xv_S8_15=S8(:,5);
Yv_S8_15=S8(:,6);
Zv_S8_15=S8(:,7);
Xf_S8_15=S8(:,8);
Yf_S8_15=S8(:,9);
Zf_S8_15=S8(:,10);

%Plot Eighth Fifteen With Optimal Traj

subplot(2,4,8)
plot3(P1, P2, P3, 'r','LineWidth',4)
grid
az=90;
el=0;
view(az, el);
xlabel('X Trajectory')
ylabel('Y Trajectory')
zlabel('Z Trajectory')

hold on

plot3(Xp_S8_15, Yp_S8_15, Zp_S8_15)
grid
az=90;
el=0;
view(az, el);
xlabel('X Trajectory')
ylabel('Y Trajectory')
zlabel('Z Trajectory')
title('Eighth Fifteen: Haptics')

end
```

REFERENCES

[1] National Stroke Association. Retrieved May 12, 2004. http://209.107.44.93/NationalStroke/default.htm.

[2] Neurology Channel. Retrieved May 12, 2004. http://www.neurologychannel.com/stroke/index.shtml.

[3] A. Vander, J. Sherman, and D. Luciano. *Human Physiology: The Mechanisms of Body Function, Eighth Edition*. New York, NY: McGraw Hill, 2001.

[4] Christopher M. Smith. *Human Factors in Haptic Interfaces*. Retrieved June 7, 2004. http://www.acm.org/crossroads/xrds3-3/haptic.html.

[5] R. Q. van der Linde and P. Lammertse. "Haptic Master – A Generic Force Controlled Robot for Human Interaction," *Industrial Robot: An International Journal*, vol. 30, number 6, pp. 515-524, 2003.

[6] StereoGraphics Corporation. Retrieved December 2, 2004. http://www.stereographics.com/products/crystaleyes/body_crystaleyes.html.

[7] OpenGL. Retrieved November 17, 2004. http://www.opengl.org/.

[8] The Mathworks. Retrieved October 25, 2004. http://www.mathworks.com/products/matlab/description1.html.

[9] J. E. Deutsch, PhD, PT, A. S. Merians, PhD, PT, G. C. Burdea, PhD, Rares Boian, PhD candidate, S. V. Adamovich, PhD, and H. Poizner, PhD. "Haptics and Virtual Reality Used to Increase Strength and Improve Function in Chronic Indiviuals Post Stroke: Two Case Reports," *Neurology Report*, vol. 26, no. 2, pp. 79-86, 2002.

[10] MIT Robot Aids Therapy of Stroke Victims. June 6, 2000. Retrieved August 31, 2004. http://web.mit.edu/newsoffice/2000/manus.html.

[11] L.R.P. Force Feedback Data Glove. Retrieved June 7, 2004. http://www.caip.rutgers.edu/~bouzit/lrp/glove.html.

[12] SensAble Technologies. Retrieved December 30, 2004. http://www.sensable.com/products/phantom_ghost/phantom.asp

[13] Sense8 Product Line. Retrieved December 2, 2004. http://sense8.sierraweb.net/products/wtk.html.

[14] H. I. Krebs, N. Hogan, B. T. Volpe, M. L. Aisen, L. Edelstein, and C. Diels. "Robot Aided Neuro-Rehabilitation in Stroke: Three-Year Follow-Up," in ICORR '99: International Conference on Rehabilitation Robotics (Stanford, CA, 1999), pp. 34-41.

[15] S. E. Fasoli, ScD, OTR/L, H. I. Krebs, PhD, J. Stein, MD, W. R. Frontera, MD, PhD, and N. Hogan, PhD. "Effects of Robotic Therapy on Motor Impairment and Recovery In Chronic Stroke," *Arch Phys Med Rehabil*, vol. 84, pp. 477-482, 2003.

[16] R. Rabkin. *Robot Helps Stroke Patients*. Columbia News Service: April 30, 2002. Retrieved August 31, 2004. http://www.jrn.columbia.edu/studentwork/cns/2002-0430/569.asp.

[17] P. Langdon, S. Keates, J. Clarkson, and P. Robinson. *Investigating the Cursor Movement Parameters for Haptic Assistance of Motion-Impaired Users*. Retrieved June 7, 2004. http://rehab-www.eng.cam.ac.uk/papers/icorr2001.

[18] S. V. Adamovich, A. S. Merians, R. Boian, M. Tremaine, G. S. Burdea, M. Recce, and H. Poizner. "A Virtual Reality Based Exercise for Hand Rehabilitation Post-Stroke: Transfer to Function," in IWVR '03: International Workshop on Virtual Rehabilitation (Piscataway, NJ, 2003), pp. 74-81.

[19] A. S. Merians, D. Jack, R. Boian, M. Tremaine, G. C. Burdea, S. V. Adamovich, M. Recce, and H. Poizner. "Virtual Reality-Augmented Rehabilitation for Patients Following Stroke," *Physical Therapy*, vol. 82, no. 9, pp. 898-915, 2002.

[20] J. E. Deutsch, J. Latonio, G. Burdea, and R. Boian. "Rehabilitation of Musculoskeletal Injuries Using the Rutgers Ankle Haptic Interface: Three Case Reports," in the EuroHaptics Conference (The University of Birmingham, UK, July 1-4, 2001), pp. 1-6.

[21] J. B. Broeren MSc, OT, M. R. Rydmark PhD, MD, and K. S. Sunnerhagen PhD, MD. "Virtual Reality and Haptics as a Training Device for Movement Rehabilitation After Stroke: A Single-Case Study," *Archives of Physical Medicine and Rehabilitation*, vol. 85, issue 9, pp. 1247-1250, 2004.

[22] R. A. Scheidt, J. B. Dingwell, and F. A. Mussa-Ivaldi. "Learning to Move Amid Uncertainty," *The Journal of Neurophysiology*, vol. 86, no. 2, pp. 971-985, 2001.

[23] J. L. Patton and F. A. Mussa-Ivaldi. "Robot-Assisted Adaptive Training: Custom Force Fields for Teaching Movement Patterns," *IEEE Transactions on Biomedical Engineering*, vol. 51, no. 4, pp. 636-646, 2004.

[24] C. D. Takahashi, R. A. Scheidt, and D. J. Reinkensmeyer. "Impedance Control and Internal Model Formation When Reaching in a Randomly Varying Dynamical Environment," *Journal of Neurophysiology*, vol. 86, no. 2, pp. 1047-1051, 2001.

[25] R. A. Scheidt, D. J. Reinkensmeyer, M. A. Conditt, W. Z. Rymer, and F. A. Mussa Ivaldi. "Persistence of Motor Adaptation During Constrained, Multi-Joint, Arm Movements," *The Journal of Neurophysiology*, vol. 84, no. 2, pp. 853-862, 2000.

[26] Personal Communication and with the Permission of Qinyin Qiu. April 18, 2005.